Physics – Uspekhi **56** (6) 539 – 564 (2013)

REVIEWS OF TOPICAL PROBLEMS PACS numbers: 42.79.Gn, 68.37.Uv, 73.20.Mf, 84.40.Ba

Optical nanoantennas

A E Krasnok, I S Maksymov, A I Denisyuk, P A Belov,
A E Miroshnichenko, C R Simovski, Yu S Kivshar

DOI: 10.3367/UFNe.0183.201306a.0561

Contents

Abstract. The field of optical nanoantennas, a rapidly developing area of optics, is reviewed. The basic concept of an optical antenna is formulated and major characteristics relevant to this structure are identified. A classification of nanoantennas into metallic and dielectric (the latter including semiconductor nanoantennas) is made. For either category, the literature is reviewed and strengths and weaknesses of different approaches are discussed. The basics of nonlinear optical antennas are outlined. Future avenues of research and application areas for the field are highlighted, and its prospects are examined.

A E Krasnok, A I Denisyuk, P A Belov St. Petersburg National Research University of Information Technologies, Mechanics, and Optics, Kronverkskii prosp. 49, 197101 St. Petersburg, Russian Federation
E-mail: krasnokfiz@mail.ru
I S Maksymov, A E Miroshnichenko Nonlinear Physics Centre, Research School of Physics and Engineering, Australian National University, Mills Road 59, Canberra ACT 0200, Australia
C R Simovski St. Petersburg National Research University of Information Technologies, Mechanics, and Optics, Kronverkskii prosp. 49, 197101 St. Petersburg, Russian Federation; Department of Electronics, School of Electrical Engineering, Aalto University, Otakaari 7, 00076 Aalto, Finland
Yu S Kivshar St. Petersburg National Research University of Information Technologies, Mechanics, and Optics, Kronverkskii prosp. 49, 197101 St. Petersburg, Russian Federation; Nonlinear Physics Centre, Research School of Physics and Engineering, Australian National University, Mills Road 59, Canberra ACT 0200, Australia
E-mail: ysk@internode.on.net

Received 28 June 2012, revised 21 November 2012
Uspekhi Fizicheskikh Nauk **183** (6) 561 – 589 (2013)
DOI: 10.3367/UFNr.0183.201306a.0561
Translated by Yu V Morozov; edited by A Radzig

1. Introduction

Antennas are important elements of wireless information transmission technologies, along with sources of electromagnetic waves and their detectors [1–6]. In radio engineering, antennas refer to devices converting electric and magnetic currents to radio waves and, vice versa, radio waves to currents [1–6]. This definition needs clarification which is certainly provided in the books cited: the induced magnetic currents are electric fields in aperture-angle antennas such as, e.g., horn antennas. The role of electric currents for such antennas is played by magnetic fields in the apertures. Notice that this classical definition of an antenna, in our opinion, is somewhat vague because the choice of antenna aperture may be arbitrary, especially for horn antennas. At the same time, this definition is sufficiently general and understandable for antennas emitting and receiving radio waves. Naturally, any system of alternating currents is to a greater or lesser extent an emitter. However, the definition of transmitting antenna implies a sufficiently high radiation efficiency, while a receiving antenna must be responsive enough to incident radio waves inducing current.

A high efficiency of current conversion to freely propagating waves (and of reverse conversion, for that matter) is achieved by optimizing the spatial distribution of the currents. Another characteristic of antennas, besides efficiency, is directivity allowing transmitting and receiving signals in a given direction. Directivity of emission (reception) makes it possible to block coupling to undesirable regions of space and concentrate the electromagnetic energy

in desirable ones. Directivity is also achieved by optimizing the spatial distribution of the currents.

Despite the long history of classical antennas, including the period of revolutionary developments in this field (1940s–1970s), the stream of scientific publications has not stopped and is even increasing. A powerful impetus to this trend is given by the progress in communication systems that currently require new types of antennas operating in the microwave or superhigh frequency (SHF) range. The same applies to SHF and ultrashort wave (USW) antennas for communication with spacecraft, including artificial satellites.

SHF and USW antennas are used not only in telecommunications but also for satellite monitoring of Earth's surface (satellite radiometry); moreover, they find a variety of other nontraditional applications, e.g., as elements of environmental sensors [7–9]. SHF antennas are successfully employed in early diagnostics and hyperthermal therapy of breast tumors (see, for instance, paper [10]). Finally, one should not to leave behind that SHF and USW antennas are important components of radars and radio telescopes. All these applications require further development of classical antennas. However, the definition of antennas with regard to these applications does not need revision.

The definition of antennas should be extended when taking into account the emergence of a new branch of science known as nano-optics, which studies the transmission and reception of optical signals by submicron and even nanometer-sized objects [11–24]. Nano-optics poses the problem of the efficiency and directivity of the transmission of optical information between nanoelements. The sources and detectors of radiation in nano-optics are nanoelements themselves, relatively small groups of them, and even individual molecules (atoms, ions) and molecular clusters. Nano-objects functioning as antennas must possess the properties of radiation efficiency and directivity.

The question is how to define antennas in this context when the notion of radiating or induced currents becomes somewhat inadequate. The term nanoantenna has been coined in the modern literature [14, 25–44]. The receiving nanoantenna is a device effectively converting incident light (optical frequency radiation) into a strongly confined field. Conversely, the transmitting antenna converts the strongly confined field in the optical frequency range created by a certain (weakly emitting or almost nonemitting) source into optical radiation. By a strongly confined field one understands an electromagnetic field concentrated in a small region compared with the wavelength of light. Such fields are characterized by a spatial spectrum containing no uniformly plane waves and consisting of a superposition of evanescent waves. The region where a strongly confined field is concentrated may by subwavelength in all three dimensions. In such a case, a strongly confined near field is created. The energy of this field comprises contributions from stored and nonradiated energy. However, an important particular case of nanoantennas is a device converting optical radiation into waveguide modes, and vice versa. In this case, the subwavelength dimension is characterized by a transverse cross section of the strongly confined field region. The longitudinal size of this region (along the waveguide axis) may be optically large, and the electromagnetic energy of the strongly confined field is referred to as expanding.

Bearing in mind the great variety of sources and detectors of strongly confined optical fields (groups of atoms and molecules, luminescent and fluorescent cells, e.g., viruses and bacteria, sometimes individual molecules, quantum dots, and quantum wires), it is safe to say that the areas of practical applications of nanoantennas in the near future will be commensurate with that of classical analogs. At present, nanoantennas are utilized in near-field microscopy and high-resolution biomedical sensors; their application for hyperthermal therapy of skin neoplasms is a matter for the foreseeable future [37, 45–55].

There are some other potential applications of nanoantennas that we believe to be equally promising. They are listed in Fig. 1. The variety of applications gives reason to argue that the concept of nanoantennas presents a unique example of the penetration of new physics into various spheres of human activity. These applications are considered in greater detail in the concluding Section 6.

The foregoing accounts for the ever-growing number of scientific publications concerned with nanoantennas. A query on the Web of Knowledge database using the keywords 'nanoantenna' and 'optical antennas' revealed that the total number of articles on nanoantennas amounted to 650 in 2011, continuing to increase at a rate of roughly 70 per year. Unfortunately, most of these papers have appeared in foreign journals, with only a few [34, 56–65] dealing with this topical issue of modern optics being found in the Russian-language literature, even though many important experimental and theoretical investigations of nanoantennas published in English-speaking journals [42, 43, 66–78] have been done by our domestic specialists. Their scientific potential appears to be sufficiently high to make a noticeable contribution to the development of nanoantennas and related research.

We hope that the present review will not only fill (even if only partly) the gap in the Russian-language nano-optics literature relevant to nanoantennas but also arouse interest in this subject among our specialists, especially young ones.

We also recommend to read the following comprehensive reviews [27, 28, 37, 41, 44] written by the leading experts in the field. References [27, 41] give an idea about the general concepts and main terms used in this field of nano-optics; they also present the relevant formulas. Reference [28] even provides a brief historical review of the development of nanoantennas, beginning from the work of E H Synge (1928) to that of J Wessel (1985) [79]. Moreover, there are

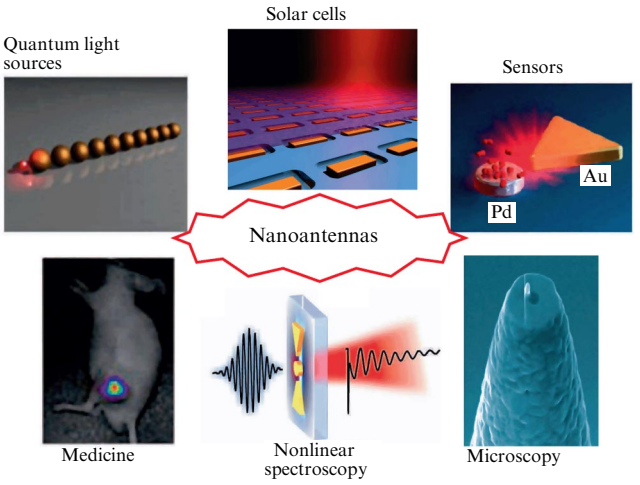

Figure 1. Plethora of nanoantennas application in modern science.

several good books on nanoantennas, including a recently published Ref. [40].

Consequently, the natural question is brought up: why not simply translate one of these review articles about nanoantennas into Russian? The answer is that our review has the advantage of being a complete one. Unlike the aforementioned authors, we do not pay much attention to details they consider to be especially interesting, but emphasize the issues that were not highlighted in previous publications. These are in the first place dielectric nanoantennas, with which we also associate nanoantennas based on semiconducting nanoparticles and hybrid (metallo-dielectric) nanoantennas. Moreover, the present review is the first attempt to systematize nanoantennas in terms of their mode of operation. Finally, many interesting studies (including experimental ones) have been done during the period since the publication of the last comprehensive reviews [27, 28]. These are included in our review even though we do not attempt to exhaustively discuss all them.

The paper outline is as follows. Section 2 is designed to provide general information on nanoantennas. It also describes the main characteristics of antennas (including nanoantennas) and introduces the system of concepts serving as the basis of this new science. Furthermore, systematization of antennas is presented in accordance with the primary objective of the review. Two major groups of nanoantennas (metallic and dielectric) are distinguished based on their functional properties. Each group is divided into subgroups. For example, metallic nanoantennas in Section 3 were categorized into monopole (Section 3.1), dipole (Section 3.2), 'bowtie' (Section 3.3), and Yagi–Uda nanoantennas (Section 3.4). The most promising applications of nanoantennas are discussed in Section 6.

2. Operation principle and main characteristics of optical nanoantennas

Summarizing the definitions of classical antennas and nanoantennas, one may say that they refer either to devices designed to effectively extract energy from an external electromagnetic field (receiving antennas) or to effectively convert localized electric and/or magnetic energy into electromagnetic radiation (transmitting antennas). The sources of radiation for transmitting nanoantennas are objects whose sizes are extremely smaller than the wavelength they emit. Such sources are called quantum emitters (hereinafter referred to as emitters). They radiate rather inefficiently due to their extremely small optical size and can not be regarded as nanoantennas. If a nanoantenna is located near an emitter, it is excited by a strongly localized emitter field, and emits an electromagnetic wave with high amplitude. Due to this, the use of the nanoantenna significantly increases the radiation power of the emitter (sometimes by a few orders of magnitude) [14–16, 18, 20–23, 80, 81]. From this perspective, a transmitting nanoantenna is a device designed to extract the energy of the emitter and convert it into sufficiently strong radiation. On the other hand, a transmitting nanoantenna, like its classical analog, has to redistribute the electromagnetic energy in space.

The aforesaid refers equally to receiving nanoantennas designed to effectively excite quantum detectors of radiation (hereinafter called detectors) that absorb only the small power of radiation incident on them due to their extremely small size compared with the wavelength. A nanoantenna creates a strongly localized field near the detector and thereby markedly enhances the power being detected. Moreover, a receiving nanoantenna has the property of directivity that depends on specific practical applications of the device. Sometimes, it is desirable to concentrate the energy to a narrow wave beam (e.g., to couple two distant emitters or an emitter and an optical fiber). Alternatively, the response of a receiving nanoantenna must be characterized by low but specific unilateral directivity; for example, the antenna must be readily excitable by the waves incoming from one half-space but poorly susceptible to the signals from another half-space. Anyway, neither the reception of an electromagnetic field nor its emission need be accompanied by massive dissipation of electromagnetic energy inside the nanoantenna.

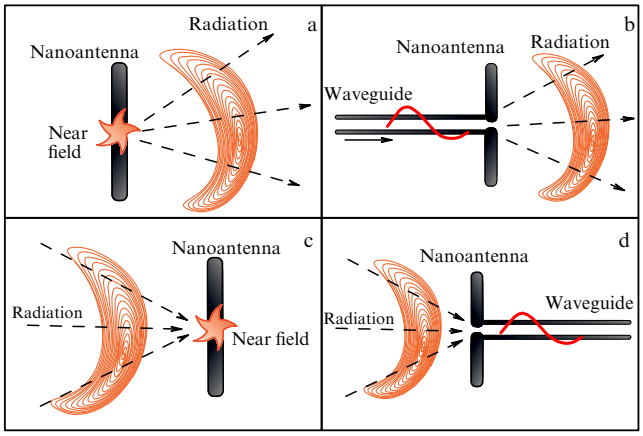

Figure 2. Principal applications of nanoantennas (exemplified by a dipole). Near field (a) or waveguide mode (b) transformation into freely propagating optical radiation; (c, d) illustrate a reception regime.

According to the principle of reciprocity [1–6], any nanoantenna may operate both as a receiver and as a transmitter. Figure 2a schematically shows the interaction between a nanoantenna and the near field of an emitter. In this case, the nanoantenna transforms the near field into freely propagating optical radiation. In other words, it is a transmitting nanoantenna. Figure 2c illustrates the operation of a receiving nanoantenna that converts incident radiation into a strongly confined near field.

The energy is usually delivered to a microwave antenna through a waveguide. Such an antenna converts waveguide modes to freely propagating radiation. In the case of optical antennas with their sufficiently small optical size, the waveguide mode must have the subwavelength cross section attainable by using so-called plasmonic waveguides [82–86]. The waveguide modes of plasmonic waveguides are characterized by enormous shortening of the effective wavelength compared with the wavelength in space. For this reason, the mode energy is concentrated in a region with a very small cross section. This type of nanoantenna feeding is depicted schematically in Fig. 2b. According to the principle of reciprocity, such a nanoantenna is also capable of transforming incident radiation to plasmonic waveguide modes (Fig. 2d). The configuration of feeding via a plasmonic waveguide is of great importance for practical applications of nanoantennas, especially for the development of wireless communication systems at the nanometer level, i.e., for future fully optical chips.

The next section introduces the main parameters that numerically characterize the operation of nanoantennas. We begin with those parameters that, on the one hand, are very general in the theory of classical radio antennas and, on the other hand, are very helpful for the analysis of optical nanoantennas.

2.1 Radiation efficiency, directivity, and gain

All quantities discussed in this section are equally applicable to both classical antennas [1–6] and nanoantennas [27, 28, 37, 41]. A nanoantenna operating as a transmitter (Fig. 2a, b) is characterized by the radiation efficiency, directivity, and gain. The characteristics of receiving antennas shown in Fig. 2c, d will be considered in Section 2.2.

Directivity. A primary characteristic of any antenna, including nanoantennas, is its directivity diagram [1–6, 27, 28, 37, 41]. The directivity diagram is a real positive function coinciding in the spherical coordinate system (θ, φ) with the Poynting vector distribution (directivity diagram in terms of intensity) in the far radiation zone ($r \gg \lambda$). This function is usually normalized to its maximum value. By way of example, Fig. 3 demonstrates the directivity diagrams of several typical systems. Not infrequently, the measurement or calculation of a three-dimensional diagram represents a difficult practical problem, especially for complex emitters. In such cases, a directivity diagram is constructed in a certain finite set of planes usually chosen based on the symmetry characteristics of the antenna's geometry. Clearly, only one such plane is needed for an isotropic emitter having a spherical directivity diagram. Two planes are sufficient for a dipole emitter due to its axial symmetry (Fig. 3a). One of the planes given by vectors **d** and **E** is called the E-plane if **d** is the electric dipole moment. The other plane orthogonal to the *E*-plane is referred to as the *H*-plane, The directivity diagram of a dipole in an *E*-plane is described by function $\mathbf{r}(\theta) \sim \sin^2\theta$, where the angle θ is counted from the direction of vector **d**.

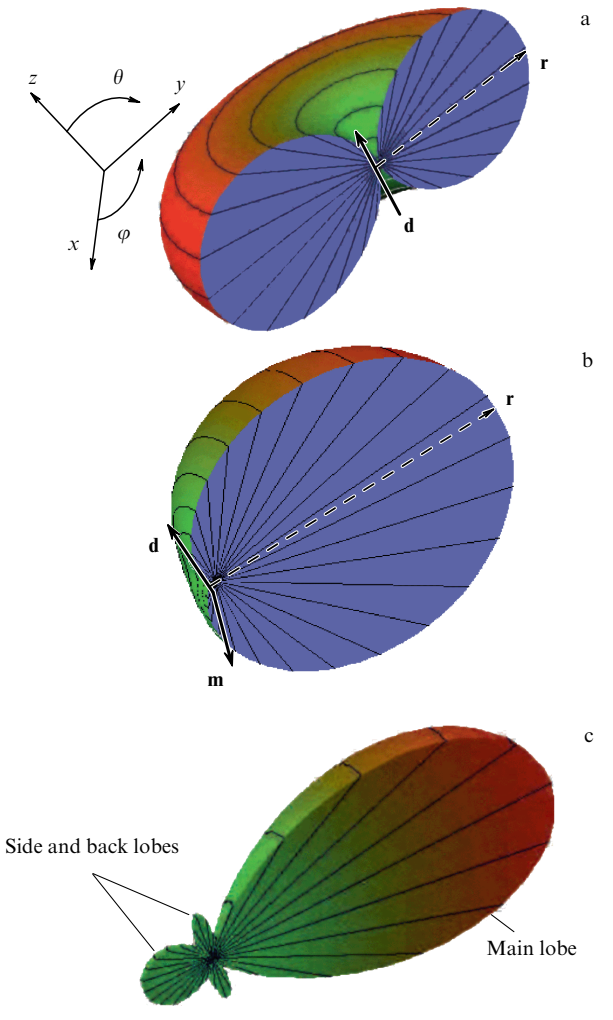

Figure 3. (Color online) Typical directivity diagrams. (a) Electric or magnetic dipole is small compared with the emitted wavelength, (b) Huygens element, and (c) Yagi–Uda antennas.

An important concept in electrodynamics and radiation theory is that of the Huygens element (see Section 4.2 for more details), i.e., the totality of two orthogonal dipole moments (electric and magnetic) undergoing phase oscillations. The directivity diagram of such an element (Fig. 3b) is axisymmetric with respect to the vector [**d m**] (i.e., identical in the *E*- and *H*-planes); it is specified by function $\mathbf{r}(\theta) \sim (1 + \sin\theta)^2$. For another relationship between the amplitudes and phases of the electric and magnetic currents, the axial symmetry of the directivity diagrams vanishes.

Figure 3c presents the directivity diagram of a typical Yagi–Uda antenna. The architecture and operation principle of such antennas will be discussed in Sections 3.4 and 4.3 below. The figure shows the position of the main, side, and back lobes inherent in the directivity diagrams of such antennas.

The concentration of radiation in a certain direction of the diagram is described by the directivity factor or simply the directivity [1–6]. The standard definition of this coefficient is given by the expression

$$D(\theta, \varphi) = \frac{4\pi p(\theta, \varphi)}{P_{\text{rad}}}, \tag{1}$$

where P_{rad} is the total power radiated by a system into the far zone, i.e., the integral of the angular distribution of the radiated power $p(\theta, \varphi)$ over the spherical surface, $\int p(\theta, \varphi)\, d\Omega$, where (θ, φ) are the angular coordinates of the spherical coordinate system, and $d\Omega$ is the element of the solid angle. The directivity factor indicates how many times the radiated power should be increased when a directional antenna is replaced by an absolutely nondirectional (isotropic) one, given that the Poynting vector modulus remains unaltered at the observation point. This expression is normalized to 4π, so that directivity of the isotropic source equals unity, and that of the dipole is 1.5

Directivity (1) is the function of the direction in space, but sometimes it is enough to know the maximum value of this quantity, namely, its value in the direction of the main lobe of the directivity diagram:

$$D_{\max} = \frac{4\pi \operatorname{Max}\left[p(\theta, \varphi)\right]}{P_{\text{rad}}}, \tag{2}$$

where $\operatorname{Max}[p(\theta, \varphi)]$ is the power transmitted in the direction of the main lobe.

Efficiency. Dissipative losses in the material of elements of a nanoantenna are inevitable during its operation. The level of these losses is characterized by the quantity called the radiation efficiency. This quantity is defined as the ratio of the power radiated by a system into the far zone to the total delivered power [1–6, 27, 37, 41]:

$$\varepsilon_{\text{rad}} = \frac{P_{\text{rad}}}{P_{\text{rad}} + P_{\text{loss}}}, \tag{3}$$

where $P_{\rm loss}$ is the total power loss in the material of the nanoantenna. For an ideal lossless antenna, one has $\varepsilon_{\rm rad} = 1$.

The radiation efficiency (3) and directivity (1) are related to one more antenna characteristic, called antenna gain [1–6, 27, 37, 41]:

$$G = \varepsilon_{\rm rad}\, D\,. \tag{4}$$

This quantity defines directivity, taking account of losses in the antennas.

However, expression (3) does not include internal losses in the emitter itself. Sometimes, it is useful to take them into consideration, making use of the so-called internal efficiency of the emitter:

$$\eta_{\rm in} = \frac{P^0}{P^0 + P^0_{\rm loss}}\,, \tag{5}$$

where $P^0_{\rm loss}$ and P^0 are the internal losses and the power radiated by the emitter in the absence of a nanoantenna, respectively. Taking account of internal losses in the emitter, the expression for $\varepsilon_{\rm rad}$ is transformed into [27]

$$\varepsilon_{\rm rad} = \frac{P_{\rm rad}/P^0}{P_{\rm rad}/P^0 + P_{\rm loss}/P^0 + (1-\eta_{\rm in})/\eta_{\rm in}}\,. \tag{6}$$

In practice, however, it is very difficult or even impossible to estimate the amount of radiation power lost in the emitter. Therefore, parameter $\eta_{\rm in}$ (5) is usually assumed to be unity, which means that an ideal emitter is considered even if it is not so under real conditions. To cope with this situation, one should remember that the term related to internal losses in the emitter and entering the denominator of formula (6) can be neglected in many important cases, while retaining the other two (much higher) terms.

2.2 Absorption cross section of a quantum detector. Field confinement factors

Quantum detectors employed in the optical frequency region have subwavelength spatial dimensions. Naturally, such small detectors are also characterized by a small absorption cross section σ equaling the ratio of the absorbed power $P_{\rm exc}$ to incident radiation intensity I:

$$\sigma(\theta, \varphi, \mathbf{n}_{\rm pol}) = \frac{P_{\rm exc}}{I}\,, \tag{7}$$

where $\mathbf{n}_{\rm pol}$ is the direction of polarization of the incident field $\mathbf{E}$.

For a detector fairly well described in the dipole approximation, the absorption cross section can be written out in the form [27]

$$\sigma = \sigma_0\, \frac{(\mathbf{n}_{\rm p}\,\mathbf{E})^2}{(\mathbf{n}_{\rm p}\,\mathbf{E}_0)^2}\,, \tag{8}$$

where σ_0 is the absorption cross section in the absence of a nanoantenna, $\mathbf{n}_{\rm p}$ is the orientation of the absorbing dipole, and $\mathbf{E}$ and $\mathbf{E}_0$ are the electric field strengths at the point of detector placement in the presence and absence of the nanoantenna, respectively. Because nanoantennas may enhance the near field in a certain space region, the absorption cross section of a detector placed in this region is also enlarged. These changes lie behind the operation principle of receiving antennas (Fig. 2c, d). A few experimental studies have demonstrated the enlargement of the absorption cross section by $10^4 - 10^6$ times [87–89].

Confined electric and magnetic field enhancement factors. Equation (8) shows that the absorption cross section of a detector depends not only on its own cross section σ_0 in the absence of a nanoantenna but also on the quantity

$$\delta^{\rm e} = \frac{|\mathbf{E}|}{|\mathbf{E}_0|}\,, \tag{9}$$

which is termed the enhancement factor of the confined electric field. This quantity marks the degree of difference between the absolute strength $|\mathbf{E}|$ of the electric field at a given point in the presence of a nanoantenna and its value $|\mathbf{E}_0|$ in the absence of a nanoantenna. This coefficient may be either greater or less than unity. For applications, certainly, it must be greater than unity by as much as possible because only in such a case does the detector efficiency increase in the presence of the nanoantenna.

There are reports in the literature [34, 42, 90, 91] suggesting the ability of nanoantennas to confine the magnetic field. Naturally, the efficiency of such nanoantennas can be characterized similarly to Eqn (9) by the enhancement factor $\delta^{\rm m}$ of the confined magnetic field:

$$\delta^{\rm m} = \frac{|\mathbf{H}|}{|\mathbf{H}_0|}\,. \tag{10}$$

This quantity has the same physical sense as $\delta^{\rm e}$. Accordingly, formula (8) for the absorption cross section of an electric dipole can be used to obtain the expression for the absorption cross section of a magnetic dipole by simply substituting $\delta^{\rm m}$ for $\delta^{\rm e}$.

The principle of reciprocity that often simplifies the solution of many problems means in particular that a nanoantenna operating as a transmitter is equally capable of acting as a receiver. In other words, its functional characteristics in the reception and transmission regimes must be related. Specifically, the application of the reciprocity theorem allows the following useful expression to be obtained [27], which establishes the relationship between the reception and transmission regimes of the nanoantenna:

$$\frac{P_{\rm exc}(\theta,\varphi)}{P^0_{\rm exc}(\theta,\varphi)} = \frac{P_{\rm rad}}{P^0_{\rm rad}}\,\frac{D(\theta,\varphi)}{D^0(\theta,\varphi)}\,. \tag{11}$$

In this expression, $P_{\rm exc}(\theta,\varphi)$ and $P^0_{\rm exc}(\theta,\varphi)$ are the powers absorbed by the detector in the presence and absence of a nanoantenna, respectively. In other words, these are characteristics of antennas operating in the reception regime. To recall, the quantity $P_{\rm exc}(\theta,\varphi)$ is the power absorbed by the detector itself distinct from power $P_{\rm loss}(\theta,\varphi)$ that equals the absorbed field power in the material of the nanoantenna. In turn, $P_{\rm rad}$ and $P^0_{\rm rad}$ are integrated powers emitted by this dipole, while $D(\theta,\varphi)$ and $D^0(\theta,\varphi)$ are directivities in the presence and absence of the nanoantenna, respectively. These parameters characterize the work of the nanoantenna in the transmission regime, while the entire expression (11) couples characteristics of the antenna operating in both regimes.

2.3 Variation of spontaneous emission rate. Purcell effect

It was noted above that a transmitting nanoantenna can significantly increase the efficiency of a quantum emitter. In this section, the mechanism of this effect is discussed.

As is known, an emitter possesses its own spectrum of allowed energy states [92]. All these quantum states are stationary, and an emitter excited into one of these states must remain in it infinitely long. However, a quantum emitter in the excited state is characterized by a finite (generally speaking, short) lifetime due to its interaction with the environment. In the simplest case of a single emitter, the surrounding medium is the free space. Of course, this interaction cannot be described in the framework of nonrelativistic quantum mechanics. This interaction leads to spontaneous transition of the excited emitter into a lower lying allowed energy state with the emission of a photon.

Before the work by E M Purcell [93] published in 1946, this spontaneous radiation was regarded as an intrinsic property of atoms or molecules. Purcell showed that the spontaneous relaxation rate of a magnetic dipole in a resonance electronic device may increase as compared with the relaxation rate in the free space, thus suggesting that the environment substantially changes the emission properties of an atom and any other quantum emitter.

Numerous publications [24, 66, 71, 94–105] dealing with this phenomenon have appeared since the first Purcell experiments, demonstrating the possibility of controling the spontaneous emission rate of an emitter in a very wide range. Later on, this effect was called the Purcell effect. Specifically, it was shown that nanoantennas represent a powerful tool with which to control the spontaneous emission rates. The spontaneous emission rate of the emitter placed in a certain heterogeneous system, γ, compared with the spontaneous emission rate in the free space, γ_0, is characterized by the Purcell factor

$$F_{\mathrm{P}} = \frac{\gamma}{\gamma_0} = \frac{P_{\mathrm{tot}}}{P^0} \,. \tag{12}$$

Naturally, the Purcell factor (12) is related to the variation of the total power P_{tot} radiated by the emitter compared to the power P^0 that the emitter radiated in the free space. That is because this process depends on the variation of the number of excitation acts and spontaneous emissions of the emitter per unit time. The total power P_{tot} is the sum of two powers: one radiated by the system, and the other absorbed in the material of the nanoantenna and its external environment.

The modern theory of the interaction of the emitter with the environment offers the following expression for the spontaneous relaxation rate [24]:

$$\gamma = \frac{2\omega_0}{3\hbar\varepsilon_0} |\mathbf{d}|^2 \rho(\mathbf{r}_0, \omega_0) \,, \tag{13}$$

$$\rho(\mathbf{r}_0, \omega_0) = \frac{6\omega_0}{\pi c^2} \left\{ \mathbf{n} \,\mathrm{Im}\left[\widehat{\mathbf{G}}(\mathbf{r}_0, \mathbf{r}_0; \omega_0)\right] \mathbf{n} \right\} ,$$

where the density of states $\rho(\mathbf{r}_0, \omega_0)$ is defined by the dyadic Green function $\widehat{G}(\mathbf{r}_0, \mathbf{r}_0; \omega_0)$ of the system at the point of quantum emitter localization, $\mathbf{n}$ is the unit vector in the $\mathbf{d}$ direction, and ω_0 is the angular radiation frequency of the quantum emitter. From the classical perspective this approach is equivalent to the electric field initially emitted by a quantum system and now returning to its source. The spontaneous relaxation rate in a free space is given by [24]

$$\gamma_0 = \frac{\omega_0^3 |\mathbf{d}|^2}{3\pi\varepsilon_0\hbar c^3} \,, \tag{14}$$

where $\mathbf{d} = \langle g|\widehat{\mathbf{d}}|\, e\rangle$ is the dipole matrix element of transition between the states $|e\rangle$ and $|g\rangle$.

Photons radiated by an emitter are absorbed by the inhomogeneous environment, e.g., a nanoantenna. For this reason, the radiative part of the Purcell factor is utilized in experimental situations:

$$\Gamma_{\mathrm{rad}} = \frac{P_{\mathrm{rad}}}{P^0} \,. \tag{15}$$

In this case, Γ_{rad} is the quantity defined through the power that escaped from the system, P_{rad}, rather than through the total power. As before, P^0 stands for the emitter radiation power in the absence of the nanoantenna.

The quantity given by Eqn (15) equals the Purcell factor F_{P} only in the absence of dissipative losses in the nanoantenna. Taking this quantity into account, expression (6) for radiation efficiency $\varepsilon_{\mathrm{rad}}$ of an ideal emitter can be rewritten as

$$\varepsilon_{\mathrm{rad}} = \frac{\Gamma_{\mathrm{rad}}}{\Gamma_{\mathrm{rad}} + P_{\mathrm{loss}}/P^0} \,. \tag{16}$$

It follows from the analysis of expression (16) that the radiation efficiency increases to unity with an increase of the radiative part Γ_{rad} of the Purcell factor, and vanishes with increasing the dissipative power loss. Moreover, the system does not radiate at all if $\Gamma_{\mathrm{rad}} = 0$. However, this effect is unrelated to the energy dissipation. As a result, it is quantity $\varepsilon_{\mathrm{rad}}$ in the form of expression (16) that characterizes the nanoantenna efficiency factor with due regard for the Purcell factor. For example, metallic nanoantennas considered in the next section operate at frequencies close to plasmon resonances and exhibit large dissipative losses. However, all of them are characterized by a very high Purcell factor, which makes it possible to obtain a considerable value of $\varepsilon_{\mathrm{rad}}$.

Dielectric nanoantennas (see Section 4) undergo significantly smaller losses in the material, but their Purcell factor is usually low. A comparison of the radiative parts Γ_{rad} of the Purcell factor in both systems points to the fact that these quantities are of the same order of magnitude.

3. Metallic nanoantennas

The history of the development of nanoantennas goes back to the work of Edward Hutchinson Synge, who was the first to suggest using metallic nanoparticles for optical field confinement in 1928. In 1985, John Wessel [79] showed that a metallic nanoparticle behaves as an antenna. He revealed that the presence of a single plasmonic particle makes it possible to overcome the diffraction limit in the resolution of optical devices and to predict their resolving power up to 1 nm. In the current literature, such nanoantennas are usually referred to as monopoles (Fig. 4), especially in the discussion of the interaction between the antennas and a quantum object. Nanoantennas of this type will be considered in detail in Section 3.1

Soon, it became clear that the strength of the near field in the gap between two or more plasmonic nanoparticles can be an order of magnitude higher than in the vicinity of an elongated nanoparticle. It is because the energy confinement in the gap occurs on smaller spatial scales. It turned out that the enhancement of the electric field in the gap between nanoparticles strongly depends on the metal used, the geometry of nanoparticles, the gap width, the radius of the curvature of the nanoparticle surface within the gap, as well as on the properties of the environment. The engineering of these parameters within a given range makes it possible to

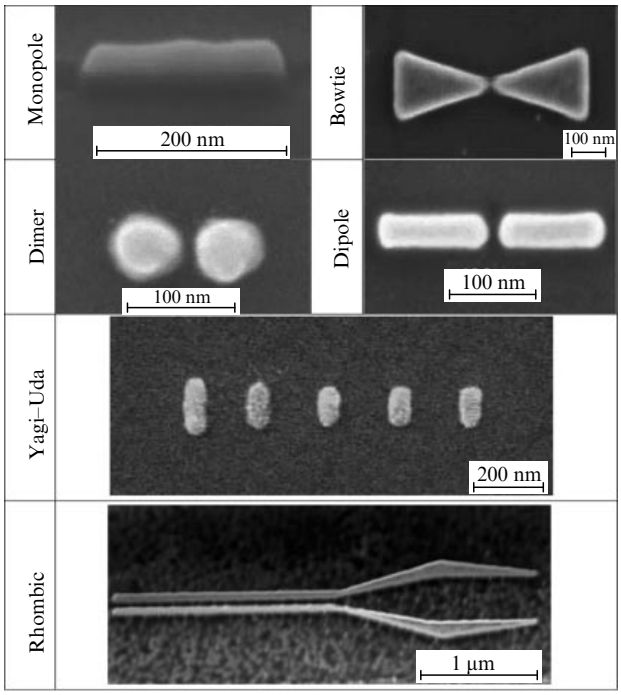

Figure 4. Main types of plasmonic nanoantennas discussed in this review.

control the position and amplitude of frequencies at which the maximum of the enhancement of the confined field strength occurs. Such a wide range of opportunities for tuning these nanoantennas and optimizing their performance in a desired regime has led to the creation of a great variety of nanoantennas having similar geometries and operation principles. The dimer nanoantennas that consist of two nanoparticles (Fig. 4) are of particular interest. This large class includes dipole nanoantennas and 'bowtie' nanoantennas, so named for their similarity to well-known garment.

The problems facing nanophotonics frequently require that a given emitter can radiate in the desired direction. This requirement is met using Yagi–Uda nanoantennas (Fig. 4). These nanoantennas are look and operate similarly to Yagi–Uda radio-frequency antennas (widely known in the Russian language literature as 'wave channel' antennas). The Yagi–Uda nanoantennas are discussed in greater detail in Section 3.4.

3.1 Plasmonic monopole nanoantennas

As mentioned above, a single metallic nanoparticle is capable of operating as a receiving nanoantenna due to its ability to enhance the electromagnetic field strength in its vicinity upon excitation of plasmon resonances of a different order. This type of a plasmonic nanoantenna is obviously the simplest and called the monopole nanoantenna. The characteristics of the monopole nanoantennas essentially depend on the shape, size, material, and dielectric environment of the nanoparticle [27, 28, 37, 41, 106]. However, these nanoantennas possess a minimum set of variable parameters and they are therefore of special importance for applications where large nanoantenna arrays and/or their high-precision fabrication are required. Figure 5a demonstrates a monopole nanoantenna operating in a radio frequency range and a monopole nanoantenna consisting of a nanowire placed on top of a substrate. In practice, however, such nanoantennas are more often fabricated as

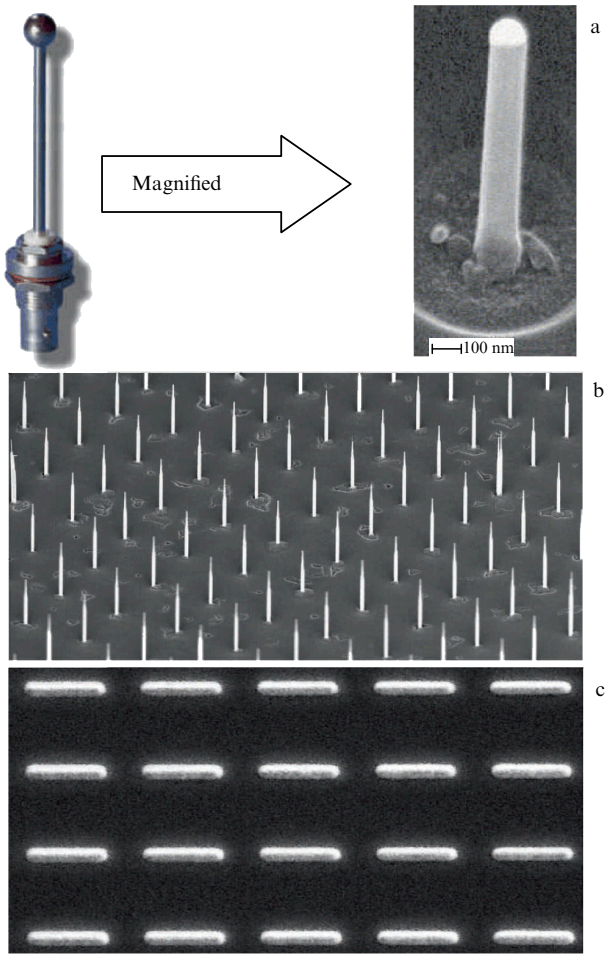

Figure 5. Monopole nanoantenna. (a) Geometric similarity of the monopole nanoantenna and its radio frequency analog. (b) and (c) Images of monopole nanoantenna arrays.

planar structures. Both types are illustrated in Figs 5b and 5c, respectively.

A plasmonic antenna excited from the far-field zone exhibits regions with highly confined electric fields. Such an enhancement of the confined field is especially pronounced in the regions of maximum electric charge density, i.e., in the parts of antennas with a high-curvature surface of the nanoelement. Experiments with such fields are usually carried out using another (probe) nanoantenna placed in this field (the method of near-field microscopy is described in Section 6.4). However, this approach is compromised by the distortion of the field studied by the probe nanoantenna. The problem is solved in different ways, e.g., by using the two-photon induced luminescence technique [107].

Figure 6 gives the results of experimental verification of the confined electric field enhancement in the immediate region of a plasmonic monopole. The figure demonstrates the level of the induced two-photon luminescence signal near the monopole (Fig. 6a) and dipole (Fig. 6b) nanoantennas. Their images were obtained by scanning electron microscopy (SEM). The nanoantennas were excited by a plane electromagnetic wave. The results for the dipole are given for the sake of comparison and they will be discussed below. The signal values in both figures are normalized to the maximum of the field in the gap of the dipole nanoantenna. It directly follows from these data that the enhancement offered by the

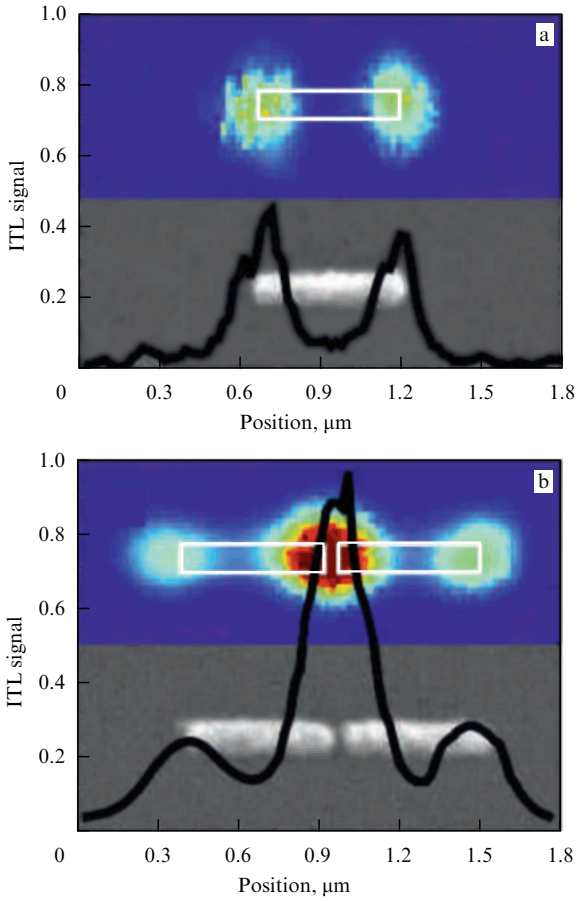

Figure 6. The level of an induced two-photon luminescence (ITL) signal near a gold nanoantenna: 500-nm long plasmonic monopole (a), and dipole consisting of two such monopoles (b). (Taken from Ref. [107].)

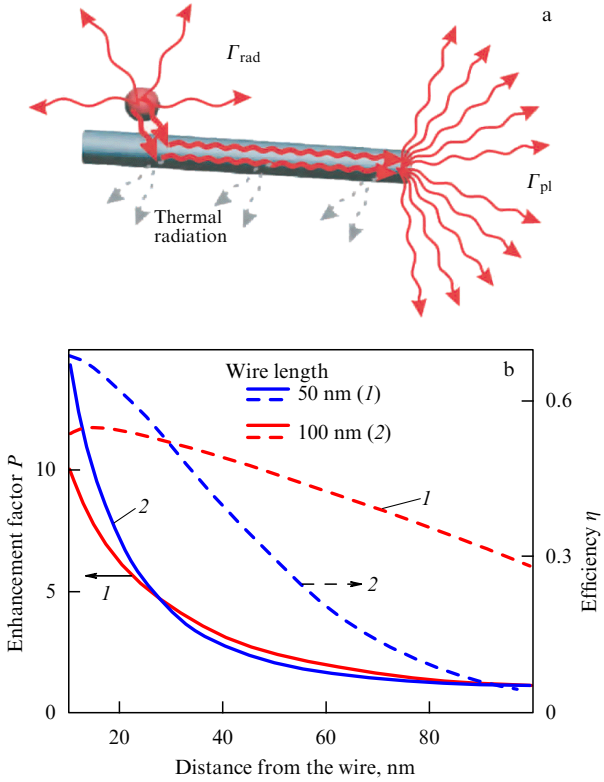

Figure 7. (Color online.) Confined field enhancement factor and radiation efficiency in the system of a plasmonic monopole interacting with a quantum dot as a function of the distance between them. (Taken from Ref. [15].)

monopole nanoantenna is smaller than that offered by the dipole nanoantenna. We note that it is difficult to judge about the field confinement factor based on these results, because it was measured from the nonlinear optical effect.

A molecule, a quantum dot, or any other detector may serve as a probe nanoantenna or nanoobject for the measurement of the near-field strength. This was convincingly demonstrated by some experimental work [15] showing that the spontaneous emission rate, i.e. the Purcell effect (see Section 2.3), of a quantum dot located near a monopole nanoantenna was increased by a factor of 2.5. Figures 7a and 7b depict the structure of the problem considered in this work and the results of numerical simulation of the system in question. They illustrate the radiation efficiency and the Purcell factor for the plasmonic monopole interacting with the quantum dot as a function of the distance between them. These data suggest that the radiation efficiency of the system rapidly decreases with increasing distance between the quantum dot and the monopole surface.

3.2 Plasmonic dimer nanoantennas. Dipole nanoantennas

Dimer nanoantennas are based on the principle of high field confinement in the gap between two metallic nanoparticles. Two subclasses of such nanoantennas exist, namely, dipole nanoantennas, and 'bowtie' nanoantennas (hereinafter 'bowties') considered in Section 3.3. Here, we focus on dipole nanoantennas and compare their performance characteristics with those of monopole nanoantennas.

Dipole configurations are widely used in radio frequency and microwave ranges as antennas proper or as reference antennas for the investigation of the properties of various emitters. They hold a unique position as being essentially the first electromagnetic antennas. Not surprisingly that analogs of such antennas also appeared in the optical range.

Although a plasmonic dipole nanoantenna represents a nanodimer, its total length is often comparable with the wavelength as, for example, in a half-wave plasmonic nanoantenna. Such devices are frequently utilized in nanoantenna technologies to build wireless (by means of freely propagating electromagnetic waves) and nanophotonic (based on waveguide modes) communication systems with the aid of optical fibers, for example, plasmonic waveguides. This is explicable on the basis of existing clearest methods of matching such nanoantennas to their feeding waveguides due to the possibility of adopting relevant techniques from radio physics [5, 6]. In this respect, dipole nanoantennas inherit the advantages of their radio frequency counterparts. The first prototype nanophotonic devices [108–110] and wireless communication systems [25, 111, 112] have been reported in the literature. However, such systems have not yet been completely realized, and their implementation is facing serious difficulties.

The idea to use dipole nanoantennas for a more efficient excitation of plasmonic waveguides was put forward in Refs [25, 111, 112]. Inspired by the works of H Hertz, the authors of paper [111] proposed a plasmonic dipole nanoantenna which is smaller in size than the wavelength of light. They showed that the introduction of materials with different permittivities in the gap of the dipole nanoantenna allows it to

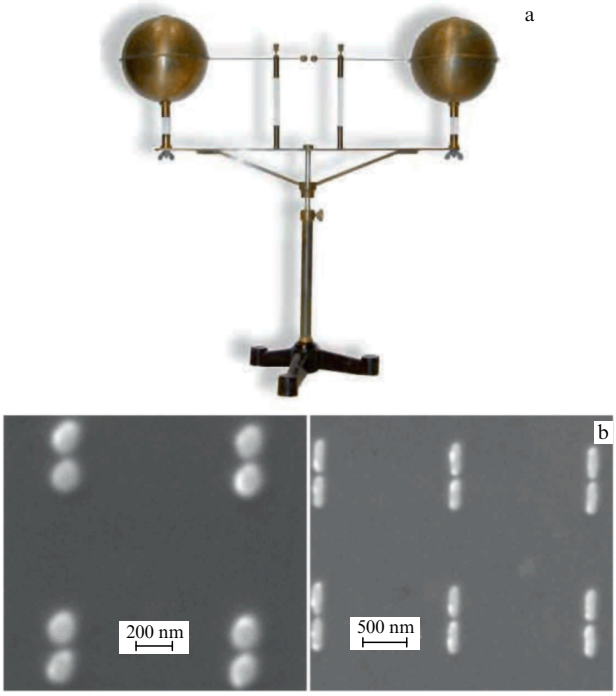

Figure 8. Dipole nanoantennas: (a) photograph of the dipole antenna used by H Hertz in his famous experiments, and (b) typical SEM images of dipole nanoantenna arrays in the form of dimers (left) and a combination of two monopoles (right).

be tuned to the desired operating regime. Both the geometry and design of such antennas make them similar to the classical Hertz dipole (Fig. 8a) that he used in his famous experiments. Figure 8b displays a typical SEM image of such nanoantennas fabricated in the form of dimers (left) and two-monopole arrays (right).

In 2008, the same authors published one more paper [112] in which they applied the input impedance concept (see, e.g., Refs [5, 6]) to analyze a plasmonic half-wave nanodipole. In other words, Ref. [112] addresses the question of nanoantenna–feeder (plasmonic waveguide) matching. The authors consider such a half-wavelength dipole nanoantenna loaded (as in the previous work [111]) with materials possessing different permittivities in its gap. It is worthy of note that the authors of Ref. [112] achieved the nanoantenna–feeder matching, i.e., demonstrated the principle possibility of the application of such a device as a transmitter or a receiver in optical wireless communication systems at the nanolevel.

The cited papers were probably the first to demonstrate coupling of nanoantennas to optical fibers. Reference [108] logically continues these studies. The authors consider a receiving nanoantenna–plasmonic waveguide–transmitting nanoantenna array (Fig. 9a) and analyze the possibility of reception of the energy from a laser beam with the ultimate goal to guide the energy in a waveguide and then couple it to the free space by means of a transmitting antenna. Specifically, they showed an excellent, if incomplete nanoantenna–feeder matching. Apparent beats of the confined field enhancement factor in Fig. 9b suggest the presence of a standing wave in the system.

Nowadays, the major body of information is transmitted over long distances through optical fiber communication lines (e.g., the Internet). However, the data received via this

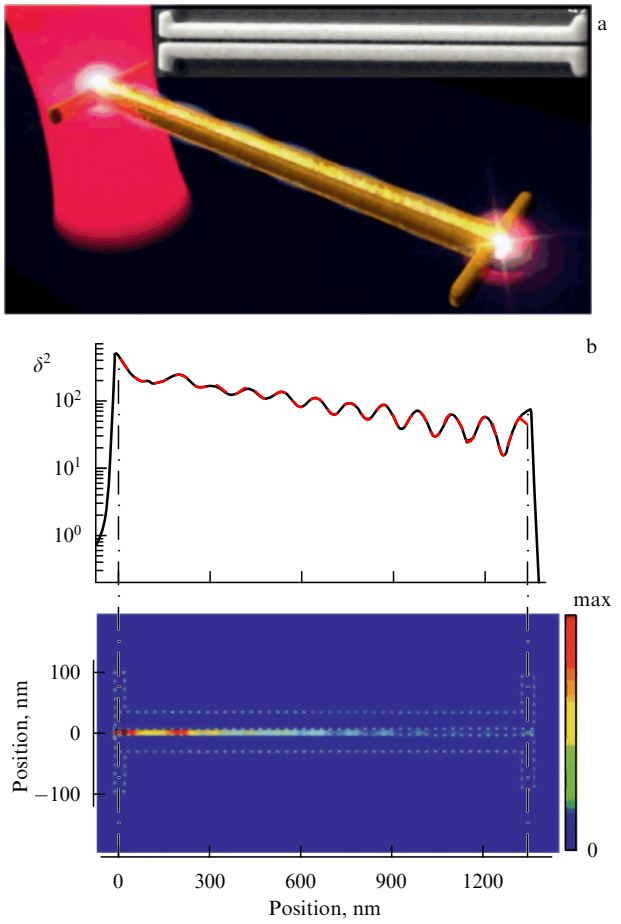

Figure 9. (Color online.) Coupling of two dipole nanoantennas via a plasmonic waveguide. (a) Design of the system consisting of a receiving nanoantenna (left), plasmonic waveguide, and transmitting nanoantenna (right). The whole structure made of gold is placed on a glass substrate. (b) Waveguide mode intensity distribution in the gap of a plasmonic waveguide. (Taken from Ref. [108].)

information channel are processed in the electronic form by converting the optical signal to an electric one. Therefore, there is a problem of coupling optical information transmission lines directly to nano-optic elements via an optical fiber bypassing electronic data processing systems. It is also proposed to address this problem with the aid of nanoantennas. The dipole nanoantenna architecture is often considered as the most suitable. Indeed, a nanoantenna directly transforming optical radiation into the waveguide plasmonic modes is the most convenient for practical purposes. The efficiency of such transformation increases substantially due to energy confinement in the subwavelength region. For example, the authors of a recently published work [109] consider this problem and propose using a plasmonic dipole nanoantenna for the coupling of light from a plasmonic waveguide to an optical fiber. Relevant numerical results are presented in Fig. 10. The comparison of Figs 10b and 10c indicates that the use of dipole nanoantennas brings substantial advantages. It is believed that such devices will help in the future to solve the problem of coupling nanophotonic systems to optical communication lines and will give rise to all-optical information transmission/processing systems.

Thus, the main advantages of dipole nanoantennas lie in the simplicity of their fabrication, the possibility of fine tuning of the operation mode, and the high confined electric field

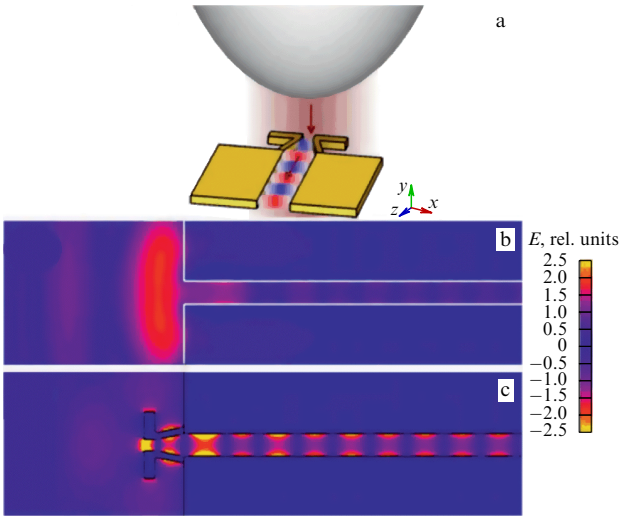

Figure 10. (a) Excitation of a plasmonic waveguide by an optical fiber mediated through a dipole nanoantenna. Comparison of confined field enhancement factors in the plasmonic waveguide with (c) and without (b) a nanoantenna. (Taken from Ref. [109].)

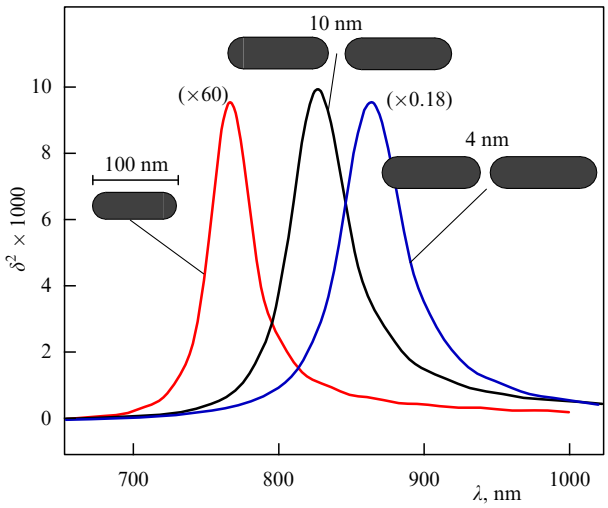

Figure 11. Comparison of the dependences of confinement factors squared for monopole and dipole nanoantennas on the exciting radiation wavelength. (Taken from Ref. [41].)

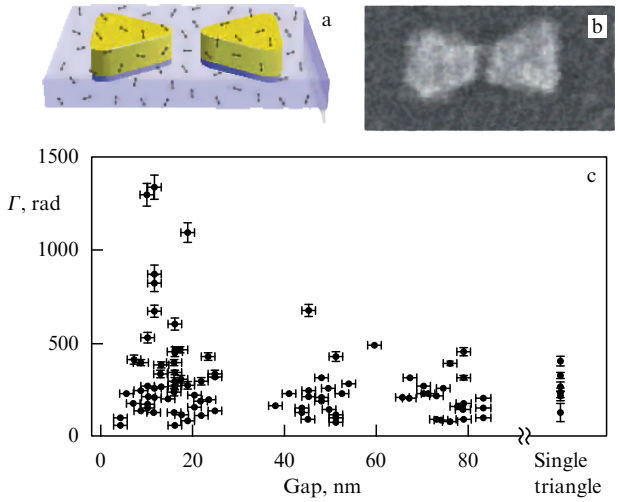

Figure 12. (Color online.) Experimental enhancement of fluorescence intensity of a molecule in the gap of a bowtie nanoantenna. (a) Bowtie design (gold). The nanoantenna is coated with dicarboximide molecules (black arrows) imbedded in methyl methacrylate (light-blue layer). (b) SEM image of the fabricated nanoantenna. (c) Dependence of fluorescence brightness enhancement of a dicarboximide molecule on the nanoantenna gap size (experimental data). (Taken from Ref. [119].)

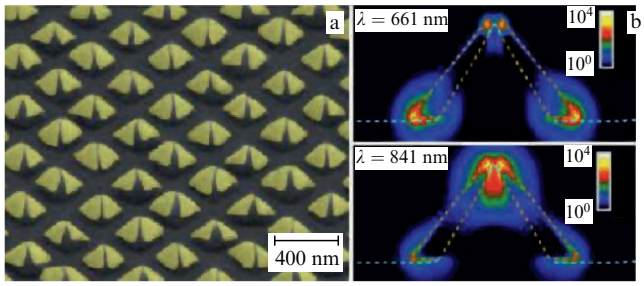

Figure 13. (a) The absorbing coating formed from an array of bowtie nanoantennas. They are arranged at an angle to the surface in order to enlarge the area of interaction with the substrate. (b) Field distribution patterns at 661 and 841 nm. (Taken from Ref. [128].)

enhancement factor in the gap, the last being much higher than in monopole analogs (Fig. 6b). Figure 11 compares the dependences of the confinement factors squared of the monopole and dipole nanoantennas on the exciting radiation wavelength [41]. Evidently, the confinement factor is significantly higher for the dipole nanoantenna than for the monopole one. Specifically, the square of the maximum value of this enhancement factor for the nanomonopole is 60 times smaller than that of a dipole nanoantenna consisting of two such nanomonopoles spaced 10 nm apart. This advantage becomes even more noticeable with decreasing gap size.

3.3 Plasmonic 'bowtie' nanoantennas

Bowtie nanoantennas [110, 113–128] represent the extension of the dimer nanoantenna model, a two-dimensional analog of classical conical radio frequency antennas (see, for instance, book [6]).

Let us start the review of bowtie nanoantennas with experimental work [119] (Fig. 12), which reports the enhancement of the fluorescence of a single molecule located in the gap of the bowtie by a factor of 10 as compared to the value obtained in previous experiments. The wavelength of 820 nm corresponded to the respective peak in the dicarboximide emission spectrum. The authors borrowed the geometric characteristics of the nanoantenna from Ref. [113]. The results of this work agree with numerical calculations. The enhanced fluorescence is attributed to the huge enhancement factor of the confined electric field (9) in the gap of the nanoantenna.

Some research groups suggest using bowties to enhance the efficiency of solar cells and to create ideal absorbing coatings. For example, the authors of experimental study [128] proposed a new design of such coatings consisting of bowtie nanoantennas placed on substrate islands rather than in the plane of the substrate (Fig. 13). This approach ensured almost complete absorption at the plasmon resonance frequency of the system largely due to enlargement of the coating area interacting with the near field.

A few recent publications aim at matching bowties to plasmonic waveguides. A receiving nanoantenna-bowtie–plasmonic waveguide–transmitting nanoantenna system was

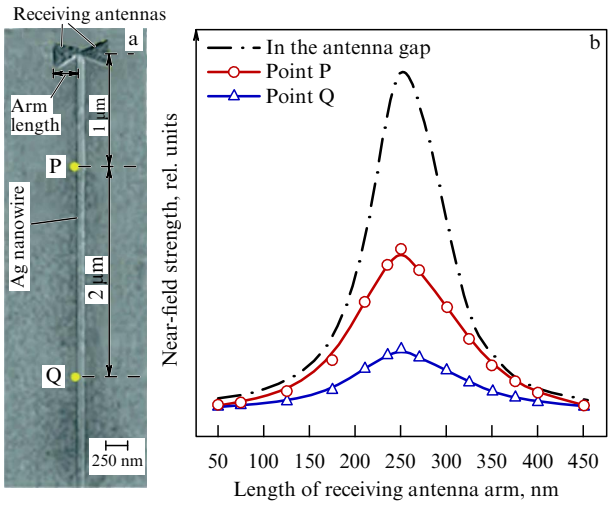

Figure 14. (Color online.) (a) Image of a receiving nanoantenna–waveguide array made of silver. (b) Electric field strength in the antenna gap (black dashed-dotted curve) and the results of measurement of near-field strength 1 μm (red circles) and 3 μm (blue triangles) from the gap of the receiving bowtie nanoantenna. (Taken from Ref. [110].)

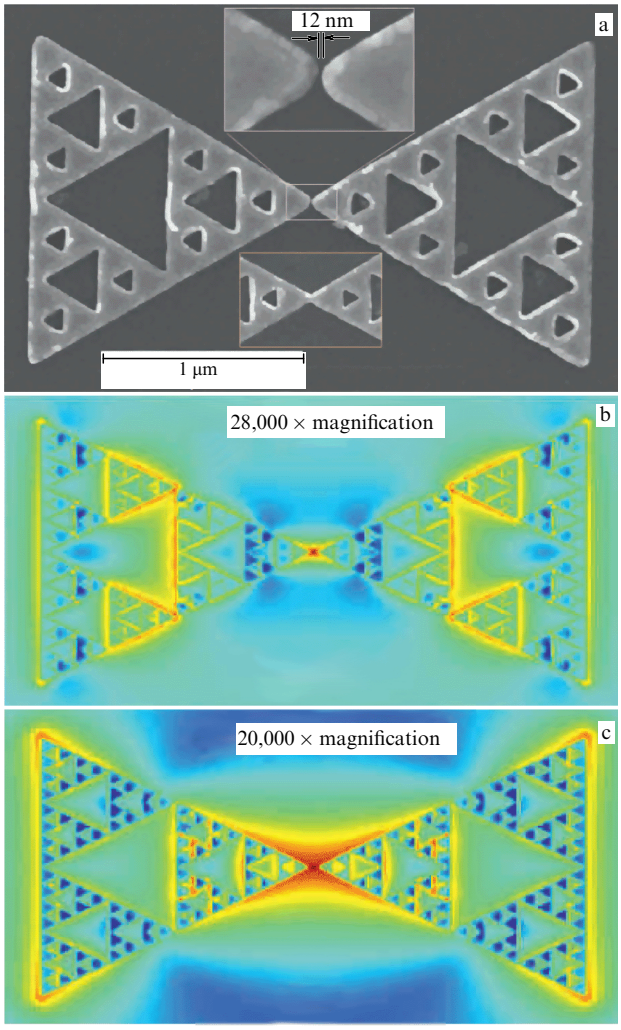

Figure 15. A bowtie nanoantenna containing Sierpinski fractal structures. Practical realization of such a device (a) and results of its numerical simulation at 2950 nm (b) and 6420 nm (c) wavelengths. (Taken from Ref. [124].)

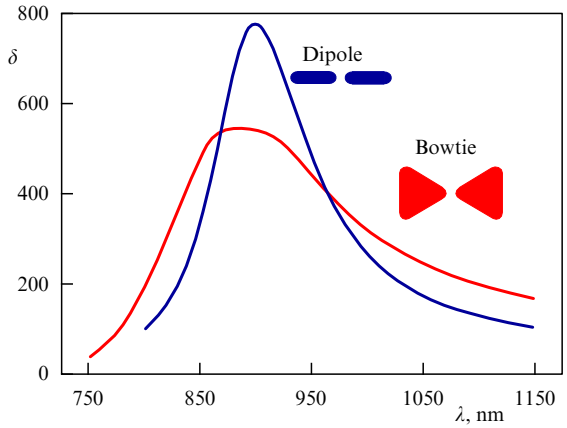

Figure 16. Comparison of bowtie and dipole nanoantennas having similar arm lengths and radii of surface curvature of the nanoelement in the gap region. (Taken from Ref. [41].)

examined experimentally in Ref. [110] (Fig. 14). Figure 14a displays only one part of the system, namely the receiving nanoantenna and the waveguide. The ends of the waveguide are positioned in the gaps of both nanoantennas. The length of the waveguide shown in Fig. 14a is 10 μm, and the arm of the nanoantenna reaches 250 nm. The receiving antenna is illuminated with a laser beam. These experiments revealed the main disadvantage of plasmonic waveguides: the rapid decay of the plasmon mode energy. It follows from Fig. 14b that the plasmon mode intensity in this waveguide significantly decreases within just 3 μm off the transmitting antenna.

An interesting idea intended to reduce dissipative losses in the material of nanoantennas and extend their operating frequency range consists in using fractal structures, such as, for example, a Sierpinski structure [124, 129]. In Ref. [124], such a structure was employed to fabricate bowties. The results of the simulation of a Sierpinski nanoantenna and a SEM image of a realistic structure are illustrated in Fig. 15. The nanoantenna operates in the infrared region. However, it is challenging to manufacture a similar but smaller nanoantenna when employing the current fabrication technologies, which is required for the operation in the visible range. This is a reason why the search is still open for other approaches to decreasing losses in plasmonic optical nanoantennas.

An important advantage of the fractal nanoantennas resides in the fact that they are relatively broadband devices inherited this property from biconical radio-frequency antennas. However, the fractal nanoantennas are outperformed by dipole nanoantennas in terms of the electric field confinement factor. This follows from the comparison of the radiation efficiency of a dipole nanoantenna and a bowtie with similar arm lengths and radii of surface curvature of the nanoelements in the gap region. The results of the comparison are presented in Fig. 16 [41]. It can be seen that albeit the operation band of bowties is broader than that of dipole nanoantennas, bowties have a lower confinement factor due to a larger amount of metal used for their fabrication and, consequently, greater dissipative losses.

Magnetic analogs of bowties have also been described. The authors of Ref. [91] propose inserting a small metal piece into the gap between nanoelements. The name Diabolo was coined, since their geometry resembles the famous toy. Figure 17a illustrates the design of the Diabolo nanoan-

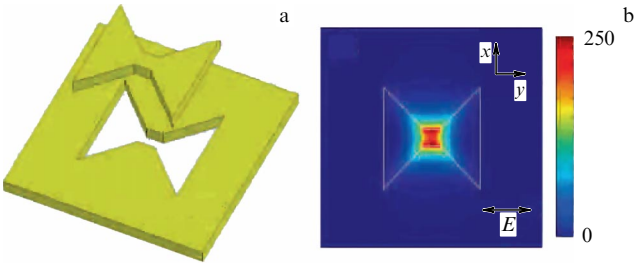

Figure 17. (a) Design of a Diabolo nanoantenna (gold). (b) Magnetic field intensity distribution at the wavelength of 1940 nm. (Taken from Ref. [91].)

tenna, and Fig. 17b presents the results of its numerical simulation, suggesting a marked rise in magnetic field intensity near the gap.

3.4 Plasmonic Yagi–Uda nanoantennas

Yagi–Uda antennas, known in the Russian language literature as wave channel antennas, are the de facto standard in the radio frequency range owing to the possibility of obtaining a narrow directivity diagram by the proper adjustment of its elements [3–6]. Suffice it to recall that Yagi–Uda type antennas are most commonly used to receive TV signals from remote stations. Figure 18a displays a photograph of Professor Hidetsugu Yagi, one of the inventors of the wave channel antenna. He holds in his hands an antenna consisting of a reflector, two directors and a feeding element. The reflector quenches backward radiation by means of destructive interference of the field scattered on it with the field of the vibrator. The directors perform the opposite function of providing constructive interference needed to form a more directed (forward) radiation [3–6].

In the realm of the modern nanophotonics, the nanoantenna should have a narrow emission pattern and also a small footprint. The latter is required for the integration of the nanoantenna with other photonic components on an optical chip. This goal is readily attained using plasmonic Yagi–Uda nanoantennas that have recently received widespread attention in the literature [28–30, 33, 35, 43, 130–139]. These devices, like radio frequency Yagi–Uda antennas, consist of a reflector and one or several directors. Their narrow directivity diagram and high gain factor, similar to those of their classical counterparts, are achievable due to the synphasic summation of the fields from different elements in a given direction. Frequently proposed designs of Yagi–Uda nanoantennas resemble the existing designs of such antennas operating in the radio frequency range. However, differences between permittivities of the metal in the radio frequency and optical ranges result in different polarizations of the elements of radio frequency and optical metallic antennas. Hence the difference in the field distributions inside and around these elements.

A complete experimental realization of Yagi–Uda nanoantennas was reported for the first time by Curto et al. [29] who demonstrated the possibility of obtaining a narrow directivity diagram. Figure 18b displays the SEM image of a nanoantenna consisting of a reflector, three directors, and an element with the quantum emitter (active vibrator) placed in its near field. The active vibrator of the nanoantenna is designed to locally enhance the electric field strength at the point where the emitter is positioned and thereby increase its radiation power due to the Purcell effect (see Section 2.3). The results of this experiment and their

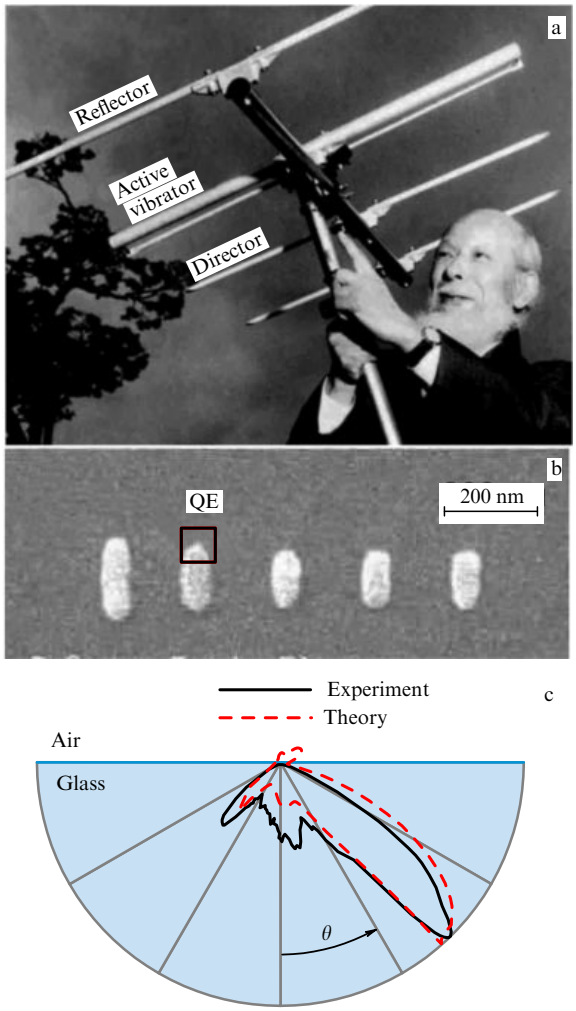

Figure 18. (Color online.) (a) A typical radio frequency Yagi–Uda antenna owned by Hidetsugu Yagi, one of its inventors, has a reflector and two directors. (b) The Yagi–Uda nanoantenna realized experimentally in Ref. [29]. (c) Results of experimental studies of this nanoantenna and their comparison with the theoretical prediction. (Taken from Ref. [29].)

comparison with numerical predictions are given in Fig. 18c. The experimental findings are in excellent agreement with numerical simulations. However, light emitted by the nanoantenna propagates largely in the optically more dense medium, i.e., the dielectric substrate. Therefore, the real directivity diagram of the nanoantenna strongly depends on the environment. Currently, this problem has not been solved and it is one of reasons why wireless optical communication between nanoantennas is a challenge.

A very recent experimental study [30] was focused on a periodic Yagi–Uda nanoantenna array (Fig. 19). Fabrication of such devices transmits the concept of antenna array from radio frequency to optical antenna technology [5, 6]. As is well known, altering the phase of each element in the array allows achieving a very high directivity. This makes it possible to scan the beam without changing the configuration of the nanoantenna. It also opens up opportunities to design adaptive antennas with directivity patterns that adjust themselves to varying environmental conditions and incoming signal direction. The creation of such devices operating in the optical range is a matter of paramount importance.

Yagi–Uda nanoantennas constitute narrowband devices that operate at the frequency determined by the dimensions of

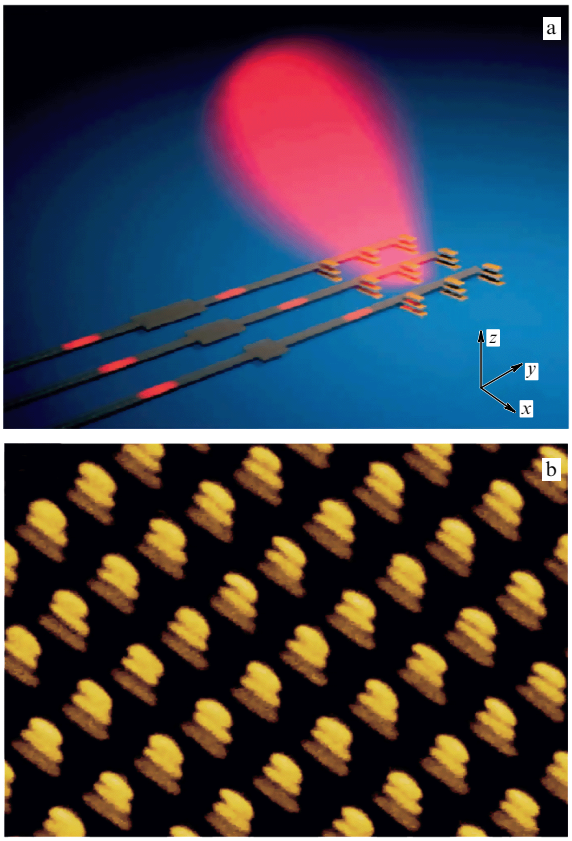

Figure 19. Phased arrays of optical nanoantennas — wave channels: (a) feed circuit of the array, and (b) SEM image of a nanoantenna array. (Taken from Ref. [30].)

the antenna elements [1–6]. The development of multiprogram TV broadcasting requires to receive several programs transmitted through various channels. Broadband antennas designed for this purpose have the ability to receive many programs with around the same efficiency. These are tapered [140], zig-zag, log-periodic, and travelling wave antennas [1–6]. Optical Yagi–Uda nanoantennas, like the majority of other plasmonic nanoantennas, are narrowband devices, since they are tuned to the frequencies close to plasmon resonances. The directivity of a nanoantenna rapidly decreases when moving away from these resonances, thus making it of little use for practical applications, most of which require broadband nanoantennas. Broadbandness in the visible region is as important as it is in the radio and TV broadcasting: a single nanoantenna must simultaneously receive several optical signals transmitted through different channels. Hence the utmost importance of further extension of the bandwidth of plasmonic nanoantennas. Moreover, broadband nanoantennas are expected to find applications in integrated optical nanochips, biosensors, solar cells, and metamaterials [77, 141–145, 151].

The miniaturization of broadband radio and TV antennas is a well-known approach to the extension of the operating waveband, and thus it can be applied to plasmonic nanoantennas. For example, the authors of Ref. [143] proposed a tapered Yagi–Uda nanoantenna consisting of director elements (nanodipoles) that shorten when moving along its principal axis (Fig. 20). The array of director elements linearly decreasing in length is needed to improve the directivity diagram of the nanoantenna and compensate for the Joule losses in metallic nanodipoles [39]. In these structures, the losses are compensated in analogy with tapered plasmonic monopole nanoantennas [20, 146, 147] by means of plasmon nanofocusing on the gradually decreasing director elements. The focusing properties can be improved by decreasing the distance between nanodipole directors to 1/50 of the wavelength of incident light. This additionally reduces the size of the nanoantenna [143] and facilitates its use with small-scale (subwavelength) emitters [77, 148]. An important feature of tapered Yagi–Uda nanoantennas consists in the possibility of controling a few subwavelength emitters, e.g., quantum dots, radiating at different frequencies or, vice versa, of receiving optical radiation coming from the far field and transforming it into subwavelength confined fields [77, 148]. Such properties are especially useful for imaging by the near-field scanning optical microscopy [149] and for multichannel wireless optical communication inside complex optical microcircuits and plasmonic solar cells (see Section 6 below).

The theoretically predicted broadband properties of tapered Yagi–Uda nanoantennas were experimentally confirmed in Ref. [143]. To this end, the authors employed electron beam lithography to fabricate two-dimensional Yagi–Uda nanoantenna arrays consisting of 21 linearly tapered gold nanodipoles. Gold was chosen in order to avoid the surface oxidation of nanoantennas observed when silver was used. The substrate was made of glass coated with a 7-nm layer of indium tin oxide. Transmission spectra of white light incident normally to the nanoantenna array surface were measured in a wide wavelength range by an optical analyzer. Spectral measurements and numerical simulation were carried out for both tapered nanoantennas and reference structures consisting of nanodipoles of equal lengths (Fig. 20b). Figures 20c–f demonstrate that experimental transmission spectra for two polarizations (parallel and perpendicular to the nanoantenna principal axis) are consistent with the results of numerical simulation.

Unlike reference structures comprising nanodipoles of equal lengths and having transmission spectra with a well-apparent resonance curve, tapered nanoantennas are characterized by broadband transmission. According to previous calculations [77, 148] and simulation of the electric field distribution in tapered nanoantennas and reference structures (Figs 20e, f), the broad transmission band is a result of the superposition of the spectra corresponding to individual nanodipoles of different lengths. In the case of reference structures consisting of equally long dipoles, Fabry–Perot resonances can be observed due to the reflection from the edges of reference structures. It is worth noting the possibility to taper both the length and the spacing between director elements of Yagi–Uda nanoantennas. Devices of this type are called optical log-periodic nanoantennas by analogy with radio and TV log-periodic antennas [114, 150, 151]. These nanoantennas exhibit broadband properties, too, but their practical realization requires much more efforts due to the enhanced demands imposed on the precision of metallic nanodipole fabrication.

3.5 Other types of plasmonic nanoantennas

The diversity of plasmonic nanoantennas is not limited to those listed in the preceding sections. For completeness, it is appropriate to overview certain plasmonic nanoantennas not included in the above discussion.

Monopole and dipole nanoantennas of a more complicated design than the aforementioned devices have also been

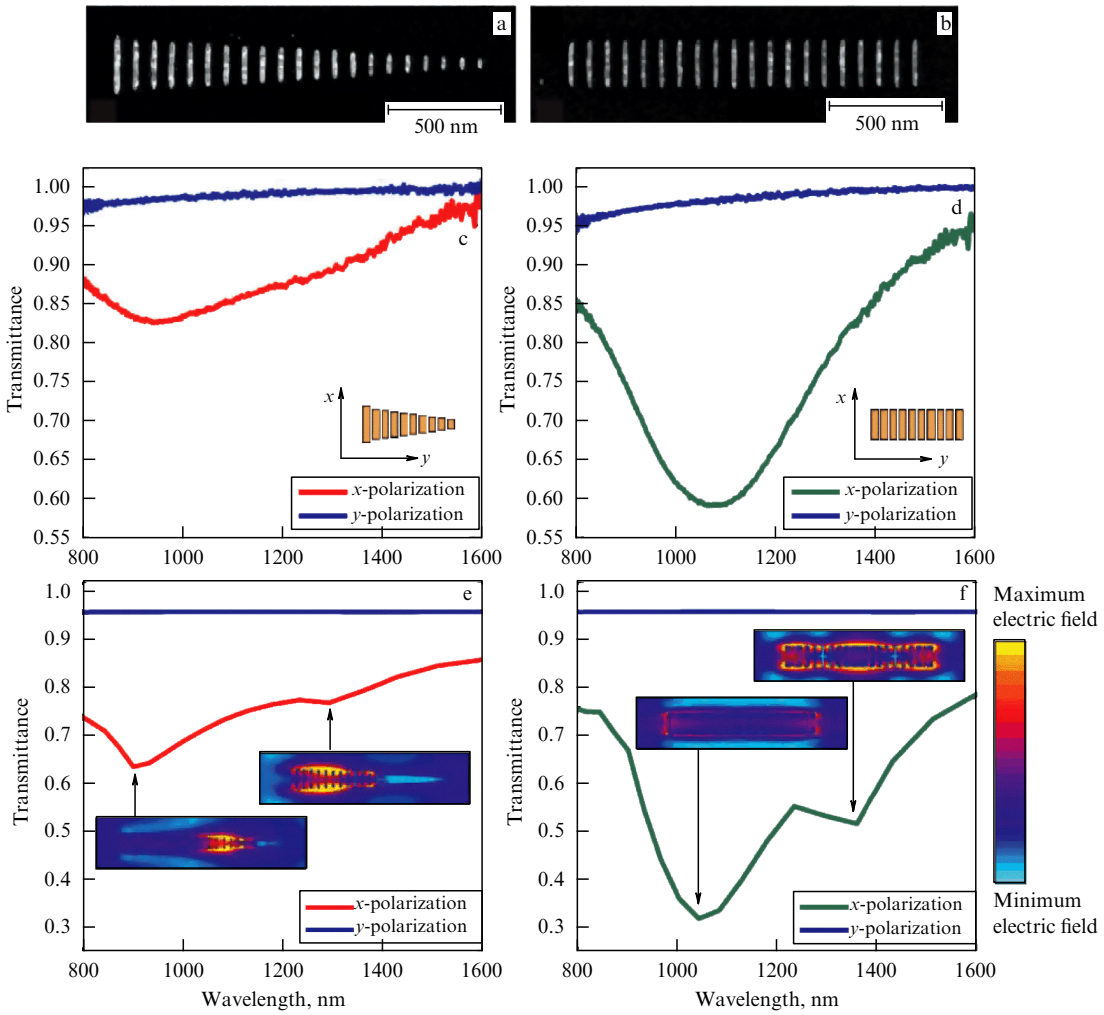

Figure 20. Tapered Yagi–Uda nanoantenna consisting of nanodipoles of different lengths. Magnified SEM images of tapered Yagi–Uda nanoantenna (a) and reference structure (b). Experimental transmission spectra of a tapered Yagi–Uda nanoantenna (c) and reference structure (d). Results of numerical simulation of transmission spectra for a tapered Yagi–Uda nanoantenna (e) and a reference structure (f). Numerically simulated electric field distributions confirm the broadband properties of tapered nanoantennas as opposed to narrowband reference structures. (Taken from Ref. [143].)

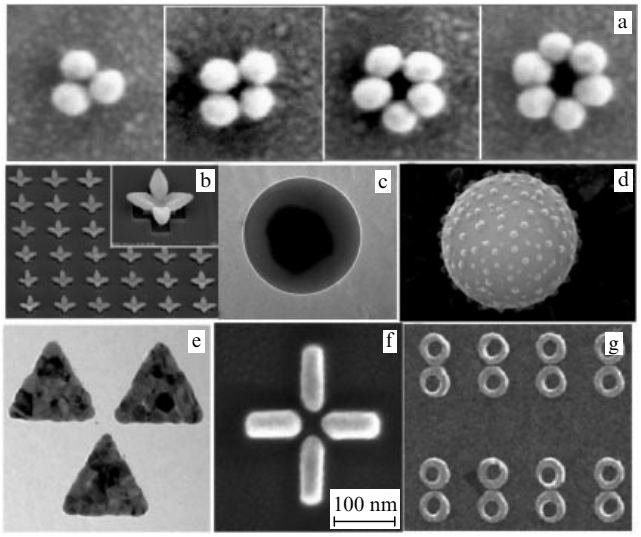

Figure 21. (Color online.) Variants of experimentally realized plasmonic nanoantennas: (a) a group of multipole nanoantennas in order of increasing multipolarity; (b) 'nanoflower' illustrating modern experimentation potential; (c) and (d) different core–shell systems, and (e–g) more sophisticated types of receiving nanoantennas.

reported in the literature [27, 28, 37, 40, 41, 152]. The difference between them reduces to the number, composition, shape, and size of the constituent nanoelements. Figure 21 exemplifies experimentally realized geometries of plasmonic monopole and dipole nanoantennas. Figure 21a depicts a group of nanoantennas that differ one from the other only in the number of nanoelements. Such multipole nanoantennas may be of interest to researchers due to the capability of supporting in them of collective plasmon modes. There are even more complex geometries. The possibilities of fabricating geometrically complicated nanoantennas are illustrated by Fig. 21b depicting a 'nanoflower' array obtained in Ref. [153].

The structural nanoelements of antennas may have an inhomogeneous composition. Figure 21c demonstrates a core–shell system made of different metals. The optical response of such systems is different from that of a homogeneous particle. Certainly, when either the core or the shell is made of a dielectric, it will be correct to classify this structure as hybrid (see Section 4 below). The structure shown in Fig. 21d has interesting optical properties. It consists of a metallic or dielectric particle and plasmonic nanoparticles of a much smaller size located on top of the larger core particle.

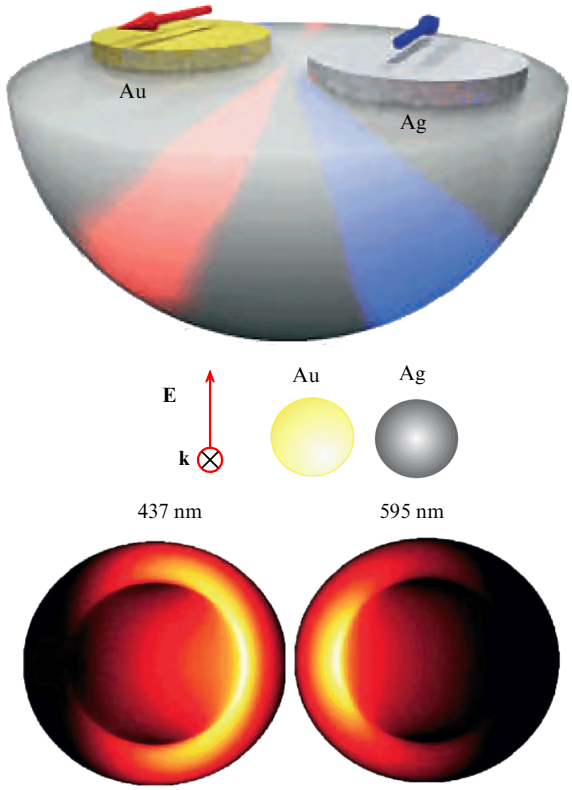

Figure 22. (Color online.) Bimetallic plasmonic nanodimer served as a directed and frequency-selective scatterer [36].

The geometries of dipole and bowtie nanoantennas may differ from those described above, as shown in Figs 21e–g. The nonstandard architectures frequently give some advantages.

Directed scatterer. Nanoscatterers, i.e., nanodevices scattering radiation in a given direction, are frequently referred to as nanoantennas. An interesting realization of the directed scatterer concept was proposed in experimental studies [36, 154]. The authors used a bimetallic nanodimer (Fig. 22), i.e., a system of coupled nanoparticles of different metals (silver and gold). The structural difference of both nanoelements makes it possible to obtain the frequency dependence of the scattered wave propagation direction. The figure shows the opposite scattering directions of red and blue color waves for the incident radiation polarized perpendicular to the dimer axis. A field polarized in a different plane is subject to a similar separation, even if at other wavelengths.

Plasmonic rhombic nanoantenna. Apart from the plasmonic Yagi–Uda nanoantennas described in the main part of this review, there are other types of nanoantennas designed to form a narrow directivity diagram. An example is a rhombic nanoantenna (Fig. 23) that is actually a plasmonic waveguide gradually widening toward the end. This type of nanoantenna is analogous to a rhombic radio frequency antenna.

Figure 23a illustrates the geometry of the rhombic nanoantenna proposed in Ref. [155], and its best directivity diagram. The authors also report results of numerical simulation of a wireless communication system between two rhombic nanoantennas. A schematic arrangement of the transmitting and receiving nanoantennas on a glass substrate is presented in Fig. 23b, and the results of numerical

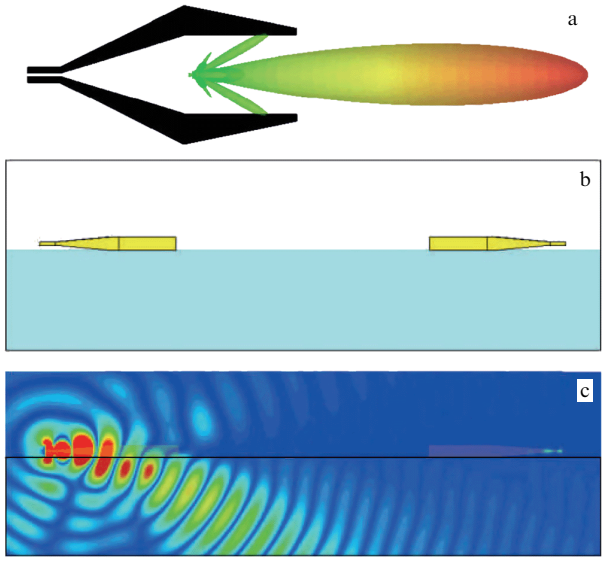

Figure 23. Rhombic nanoantenna: (a) design and directivity diagram; (b) arrangement of two nanoantennas on a glass substrate, and (c) results of numerical simulation of a wireless system for data transfer between two rhombic nanoantennas. (Taken from Ref. [155].)

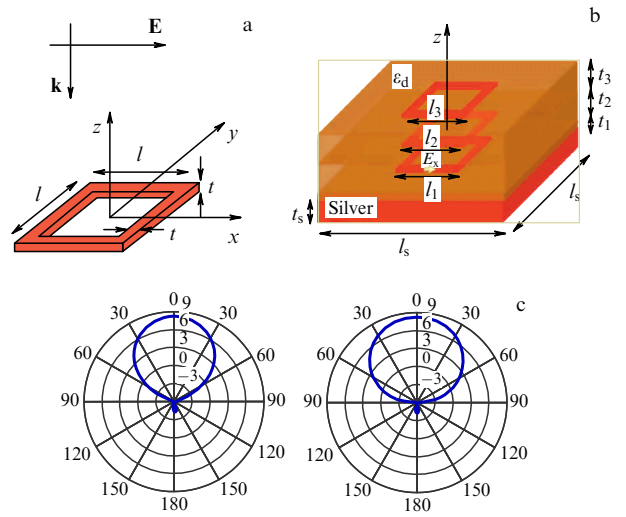

Figure 24. (a) Design of a plasmonic ring ($l = 85$ nm, $t = 15$ nm). (b) Array of isolated plasmonic rings; the ring closest to the substrate is open. The source is an emitter located in this gap along the x-axis. Excitation wavelength is 1.34 μm. (c) Directivity diagrams of plasmonic ring array in E- and H-planes, respectively. (Taken from Ref. [90].)

simulations in Fig. 23c. Obviously, a *major part of the power* radiated by the antenna also enters the substrate. Rhombic nanoantennas are difficult to find in the literature and they seem to be less interesting to researchers than the Yagi–Uda design.

Plasmonic loop nanoantenna. Not only electric dipole nanoantennas but also their magnetic-dipole counterparts are described in the literature. For example, the authors of Ref. [90] propose using an array of small plasmonic rings as a nanoantenna (Fig. 24a). It is shown in the paper cited that such a single ring has a plane wave scattering diagram in the form of a radiation directivity diagram of a magnetic dipole. Figure 24b depicts a ring array excited by a dipole located in the gap of the ring closest to the substrate. Figure 24c displays the directivity diagram of such a nanoantenna. It is worth

noting that such high directivity is due not only to the ring array but also to the back reflecting surface (silver). An obvious advantage of this type of nanoantenna is the possibility of working at one of the communication wavelengths. A disadvantage reduces to the impossibility of transferring the plasmonic ring magnetic resonance frequency to the visible frequency range [18].

Obviously, plasmonic nanoantennas continue to improve and new designs are proposed from time to time. However, the drawbacks of nanoantennas, including high energy dissipation, motivate to the search for new solutions. Besides the search for more advantageous plasmonic geometries, publications in the scientific literature are concerned with the application of the optical response properties of dielectric nanoelements. Such nanoantennas are referred to as dielectric, and include semiconductor nanoantennas as well. These nanoantennas are considered in the next section.

4. Dielectric nanoantennas

Nanoantenna designs taking advantage of the optical response of dielectric and semiconducting particles have appeared in the last few years in Refs [31, 34, 42, 70, 74, 156–170], in addition to metallic (plasmonic) nanoantennas. Unlike metallic nanoantennas made from an opaque material having plasmonic properties in the optical range, dielectric nanoantennas are fabricated from optically transparent materials. Their resonant response is related to the formation of an effective resonator inside the particle. The antennas based on semiconducting particles are also called dielectric nanoantennas, because semiconductors are sufficiently transparent in the visible frequency range. As of the date of issuing this review, the number of publications on dielectric nanoantennas is much smaller than on plasmonic ones. The dielectric nanoantennas compose new research direction and thus they are still in their infancy.

Most of the works on dielectric nanoantennas consider spherical particles [34, 42, 70, 74, 156–161, 163, 164, 169–171], and only some of them consider rods and disks [31, 162, 165, 167, 168]. However, a major portion of dielectric antennas proposed in these articles can hardly be regarded as nanoantennas, even though their operating frequency range falls into the optical region. This is because most of them are more than 1 μm in size. In what follows, therefore, we overview the works on submicron particles only.

Why are dielectric nanoantennas of interest to researchers? First, dielectric and many semiconductor materials are characterized by notably low dissipative losses in the optical range. Second, there is a wavelength range in which a submicron dielectric particle of silicon (a material with high permittivity) simultaneously exhibits electric and magnetic resonant responses [76, 172]. It makes possible the creation of the Huygens element using a single particle [5, 6]. This effect is of primary importance to optics. Due to the directional properties and low losses, Huygens-element particles can be utilized to construct compact dielectric nanoantennas with very high directivity, such as, for instance, Yagi–Uda nanoantennas.

Moreover, many light-trapping nanostructures [173–177] comprise ordered combinations of dielectric and semiconducting nanoelements that can be classified as receiving dielectric nanoantennas.

This section presents a review of all physically meaningful works on dielectric and hybrid nanoantennas containing dielectric and metallic particles. We start with all-dielectric nanoantennas as an alternative to plasmonic nanoantennas. First, we consider the geometrically the large whispering mode nanoantennas (Section 4.1). Then we move to the novel concept of nanoantennas (Section 4.2) which involve two dipole (electric and magnetic) Mie modes and operate in the Huygens element regime [34, 42, 70, 74]. Finally, we shall show that this regime opens up new opportunities for the development of high-directivity antennas and switching nanoantennas.

4.1 Whispering gallery antennas

The electrodynamics of dielectric microspheres has well-known solutions in the form of eigenmodes termed whispering gallery modes. They are resonant standing waves which can be excited in axisymmetric systems due to total internal reflection effect. Whispering gallery antennas involving dielectric microspheres possess good directional capabilities by virtue of their large surface area, i.e., radiating aperture. A most serious drawback of such nanoantennas is that they have a weak influence on the spontaneous relaxation rate of the emitter.

Here, we mention only Ref. [161], where it is shown experimentally that a single dielectric microsphere can enhance the intensity of excitation of one molecule more than twofold. In this case, such a microsphere efficiently concentrates the radiation into a narrow beam, which additionally increases intensity at the reception point. The 60% increase in the radiation intensity due to narrowing of the directivity diagram was reached in paper [161] with an almost fivefold rise in the total number of collected photons. Figure 25a presents simulated distribution of the radiation electric field of a molecule located above the surface of a

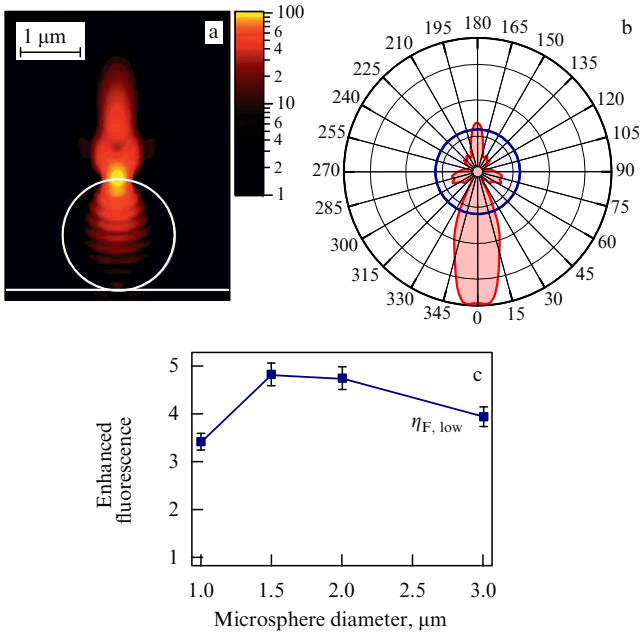

Figure 25. (Color online). (a) Simulation of electric field distribution for a single fluorescent molecule located above the surface of a dielectric microsphere. (b) Radiation directivity diagram averaged over various molecule orientations [blue (solid) curve — directivity diagram in the absence of the microsphere]. (c) Experimental data suggesting enhanced fluorescence at the observation point, depending on microsphere diameter. (Taken from Ref. [161].)

dielectric microsphere 2 μm in diameter with a refractive index of 1.59. The figure shows a rather strong field at the point of molecule location, hence the enhanced spontaneous emission rate of the system.

Experimental study [161] confirms that the Purcell factor (12) of such systems is usually small. For this reason, these systems are often combined at present with plasmonic particles [156–158, 178], such as plasmonic nanodimers, with radiating atoms, molecules, or quantum dots introduced into their near field. This combination ensures both the high Purcell factor and the good spatial directivity of radiation due to the large aperture of the dielectric microsphere. Such nanoantennas are no longer purely dielectric or metallic structures; they are considered in the concluding part of the review.

4.2 Huygens element

This section dwells on the concept of the Huygens optical element for the creation of totally dielectric nanoantennas [34, 42, 70, 74, 169, 170]. By the Huygens element is meant a dielectric particle of material with high permittivity (on the order of 10–20) due to which it has the first two Mie resonances, electric and magnetic, in the visible frequency range. Excitation of such a dielectric particle by an emitter induces in it electric and magnetic dipole moments. At certain frequencies depending on the material and the size of the nanoparticle, the amplitudes of electric and magnetic polarizabilities are equal to each other. Given polarizability phases are identical in this case, too, such a system has a radiation or scattering directivity diagram in the form of a cardioid, i.e., has the properties of the Huygens element (Fig. 3b). We demonstrate below that this permits creating compact fully dielectric nanoantennas with good directional properties, remaining in the framework of the entirely dielectric approach.

The authors of Refs [172, 179–182] noticed that there is a wavelength range in which a dielectric particle (not necessarily a nanoscale one) of a material with high permittivity may simultaneously exhibit electric and magnetic responses. Specifically, electric and magnetic polarizabilities of a spherical dielectric particle are defined in the dipole approximation by the expressions $\alpha^{e} = 6\pi i a_1/k^3$ and $\alpha^{m} = 6\pi i b_1/k^3$, respectively, where coefficients a_1 and b_1 are the scattered field amplitudes in the first (dipole) approximation [183].

There are various dielectric materials with a rather large real part of permittivity in the optical range, which simultaneously have a low level of dissipative losses. They are exemplified by silicon (Si, $\varepsilon_1 = 16$), germanium (Ge, $\varepsilon_1 = 20$), aluminum antimonide (AlSb, $\varepsilon_1 = 12$), aluminum arsenide (AlAs, $\varepsilon_1 = 10$), and many other compounds. Their permittivity values are such that they allow nanoparticles to have electric and magnetic Mie resonances in the visible frequency range.

The authors of Refs [34, 42, 70, 74] consider the dipole–silicon nanoparticle system depicted in Fig. 26a. A spherical dielectric silicon nanoparticle is placed in the near field of an elementary dipole. The real part of silicon permittivity in the visible frequency range roughly equals 16 [184], and dissipative losses in silicon are lower than in a precious metal (gold or silver). The maximum radius of the silicon particle satisfying the dipole approximation in the optical range approximately equals 80 nm. The aforementioned studies revealed the wavelength region in which such a silicon particle exhibits the properties of the Huygens

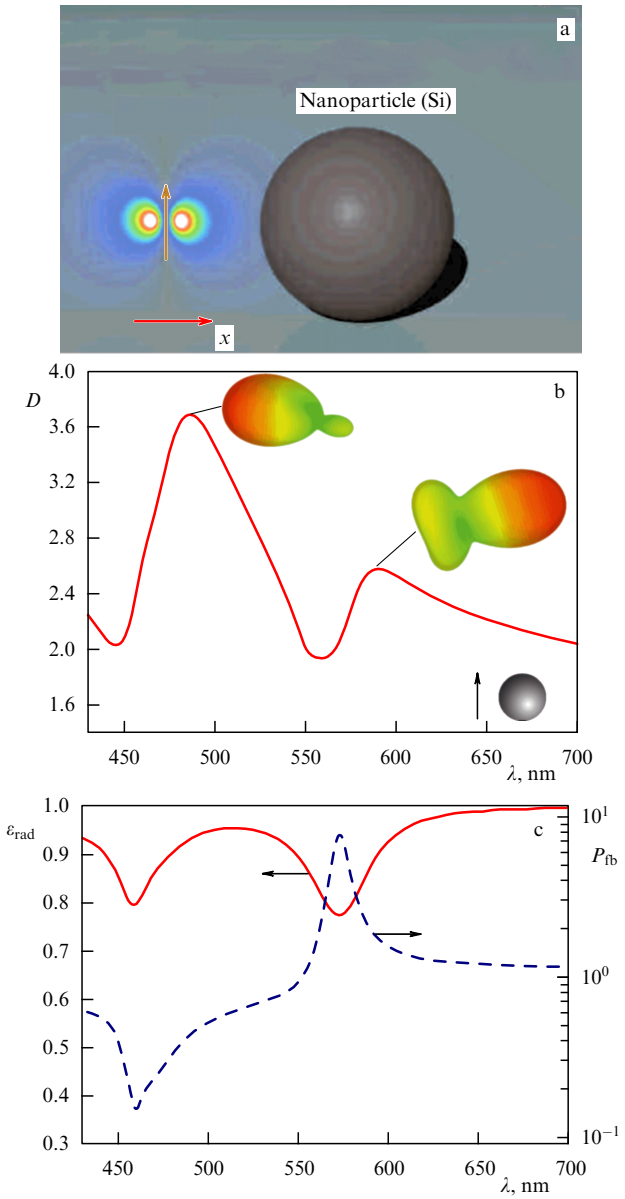

Figure 26. (Color online.) (a) Huygens element. (b) Wavelength dependence of directivity factors. Insets show 3D directivity diagrams. (c) Wavelength dependences of radiation efficiency (red solid curve, left-hand linear scale) and forward/backward radiation ratio (blue dashed curve, right-hand logarithmic scale). (Taken from Refs [34, 70].)

element. Moreover, the wavelength dependence of oscillation phases of the particle's electric and magnetic moment vectors makes it possible to switch the main direction of the directivity diagram between two directions (forward and backward).

Figure 26b depicts the wavelength dependence of the directivity factor in such a system. The insets demonstrate 3D directivity diagrams at the respective frequencies. The diagram's main lobe is differently directed in these two cases, viz. toward the negative side of the x-axis at 480 nm, and toward its positive side at 590 nm. The operating regime turns over at a frequency of 550 nm, corresponding to a magnetic dipole resonance. Figure 26c presents radiation efficiency ε_{rad} (solid curve) and the ratio of power P_{fb} radiated in the positive (forward) direction of the x-axis to the power radiated backward. The efficiency curve confirms the afore-

mentioned possibility of obtaining small dissipative losses in dielectric nanoantennas.

4.3 Dielectric Yagi–Uda nanoantennas

The properties of a single dielectric nanoparticle with high permittivity described in the preceding section can be used to design nanoantennas with good directional characteristics. The authors of Refs [34, 42, 70, 74] elaborated the concept of the Huygens optical element expounded in Section 4.2 for the development of a totally dielectric Yagi–Uda nanoantenna. They added four more dielectric nanoparticles of equal size to the system illustrated in Fig. 26a (see Fig. 27a). Figure 27b presents the wavelength dependence of the directivity factor for a dielectric nanoantenna (wave channel); the distance (G) between the director surfaces measures 70 nm, whereas the reflector and the first director are spaced $2G$ apart. The insets display 3D directivity diagrams at respective frequencies. It can be seen that the dependence has a sharp maximum at 500 nm. The main lobe of the diagram became markedly sharpened, while backward radiation is virtually absent. It is the functioning of each dielectric sphere as the Huygens element (the presence of electric and magnetic moments) that gives rise to such a directivity diagram. Figure 27c presents wavelength dependences of radiation efficiency for different values of parameter G. The radiation efficiency of dielectric Yagi–Uda nanoantennas slowly decreases with decreasing distance between the elements; on the other hand, it remains practically unaltered at wavelengths corresponding to the directivity factor maxima. It was shown in Ref. [70] that the operational regime of a dielectric Yagi–Uda nanoantenna strongly depends on the distance between the elements. It has, in turn, a marked effect on the directivity factor. The contribution of the particles' electric moment to the directivity factor decreases as the space between the nanoelements becomes smaller; conversely, the contribution from the magnetic moment increases. As a result, the nanoantenna gradually moves to the 'magnetic' operational regime, in which it has the best directivity at the frequencies near nanoparticle's magnetic resonance.

This brings up a question about experimental verification of numerical simulations and theoretical interpretations of the properties of dielectric nanoantennas. Setting aside questions concerning the purely quantum properties of the source, such a verification can be realized by scaling the dielectric Yagi–Uda nanoantenna to the microwave region. A crucial point here is the inverse dependence between Mie resonance frequencies and the radius of a dielectric particle at constant permittivity of the particle material.

Reference [42] reports the results of experimental verification of the concept of dielectric nanoantennas (wave

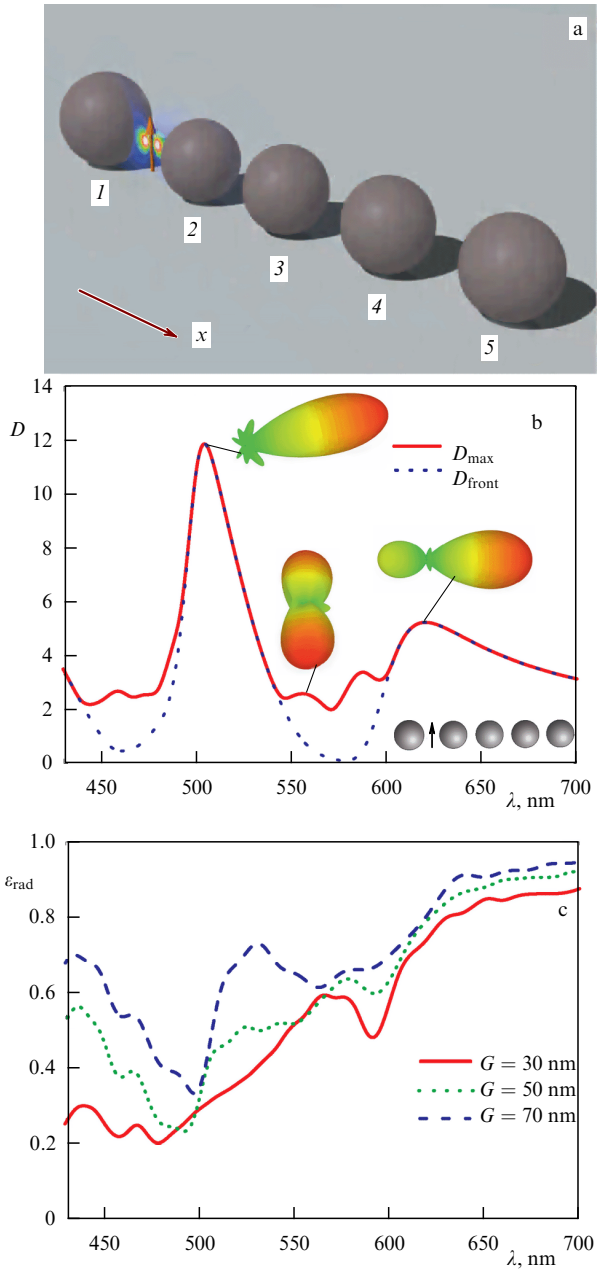

Figure 27. (a) Totally dielectric Yagi–Uda nanoantenna. (b) Wavelength dependence of directivity factor for dielectric Yagi–Uda nanoantenna, with $G = 70$ nm. Insets show 3D directivity diagrams at respective frequencies. (c) Wavelength dependences of radiation efficiency for different values of parameter G. (Taken from Refs [34, 70, 74].)

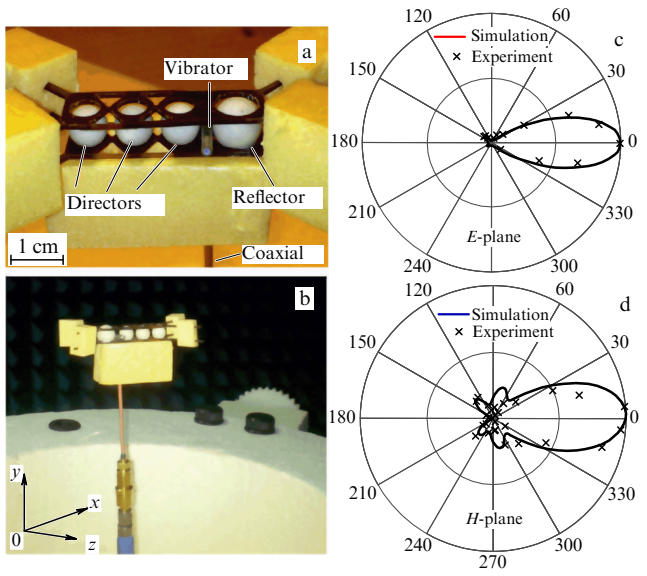

Figure 28. Dielectric Yagi–Uda nanoantenna together with its fasteners (a) and the arrangement of the entire device in an echo-free dark room (b). An y-axis of the coordinate system is directed along the vibrator axis, and x-axis along the antenna axis (c, d). Directivity diagrams in E- and H-planes, respectively. (Taken from Ref. [42].)

channels) (Fig. 28) in the microwave radiation region by the frequency scaling technique; they were compared with the results of numerical simulations. Dielectric spheres were made from $MgO-TiO_2$, a microwave ceramic having a permittivity of 16 in the frequency range of interest (i.e., equal to that of silicon in the optical range [184]). Figure 28c, d presents directivity diagrams of the nanoantenna in *E*- and *H*-planes, respectively, obtained experimentally at 10.7 GHz. It can be seen that the experimental data are in excellent agreement with numerical calculations, while some discrepancy is attributable to the presence of fasteners. This work confirms the validity of the main operating principles of dielectric Yagi–Uda nanoantennas.

Hybrid nanoantennas. Studies of plasmonic nanoantennas suggest a high level of their dissipation losses, especially when the distance between metallic nanoelements is smaller than their characteristic size. In this case, strongly dissipative higher-order plasmon modes are excited in a system of interacting metallic nanoparticles. Dielectric nanoantennas allow obviating this problem, but their Purcell factor is usually small. The authors of Refs [156–158, 178] proposed a design of hybrid nanoantennas free from these drawbacks by way of the rational combination of dielectric and metallic nanoelements within a single device.

The authors of Ref. [158] proposed an efficient hybrid metallic–dielectric nanoantenna (Fig. 29) combining the advantages of dielectric and metallic nanoelements. This antenna consists of a pair of metallic nanoparticles that serve to enhance the spontaneous emission rate of an emitter placed between them, and a dielectric (TiO_2) microsphere needed to effectively collect radiated light into a narrow beam. Notice, however, that the size of the sphere is several times that of the particles used in Refs [34, 42], and it operates at higher-order Mie resonances.

This work convincingly demonstrates that a combination of good directive properties of the dielectric microsphere and the ability of metallic nanoparticles to significantly enhance the confined field at plasmon resonance permits achieving both high values of the Purcell factor and the required directivity diagram. Concluding, the authors of Ref. [158] believe that the use of even larger spheres, in which whispering gallery modes may arise in the visible frequency range, will open up possibilities for the development of hybrid nanoantennas with a higher Purcell factor and directivity coefficient.

There are more publications in the literature, besides Ref. [158], concerning hybrid structures employed for practical purposes, although they are not nanoantennas proper. By way of example, the authors of Refs [156, 157, 178] propose a design of an optoplasmonic superlens based on a rather big dielectric microsphere of radius 2.8 μm having a refraction index of 1.59. The main result of this work consists in the achievement of efficient coupling between two points in space with high electric field confinement. The strong near field passes from one point to another through the dielectric microsphere. Such elements provide a basis for many nanophotonic devices transmitting information via the near field.

5. Nonlinear optical nanoantennas

The work with nanoantennas and the development of nanoantenna-based nanophotonic devices imply the possibility of controling their operating characteristics, such as the working bandwidth and the confined field enhancement factor. Such a requirement ensues in the first place from the fact that the process of fabricating nanoantennas and their arrays is fraught with errors resulting, for example, in the emitter luminescence frequency running out of the nanoantenna's working bandwidth. Second, the conditions of nanoantenna operation may vary in time, e.g., as a result of heating the antenna itself or the underlying substrate. Finally, the possibility of controling operating characteristics of nanoantennas enables the development of various nanophotonic devices, such as nano-optical switches, allowing one to choose the direction of the main lobe of the directivity diagram or the working frequency from the emitter radiation spectrum with a complicated system of stationary states. This is true of transmitting nanoantennas.

As far as receiving nanoantennas are concerned, they provide ample opportunities for controling both the position of detector's absorption cross section maxima and their width or magnitude. Therefore, nanoantennas for practical applications are designed so as to be able to change their operating characteristics in a certain frequency range and respond to external action in the desired manner. In other words, nanoantennas must be active devices. Bearing in mind their extremely small size and working frequencies, the most evident and rational method for the fabrication of active nanoantennas appears to be the introduction of a nonlinear optical response into their operation.

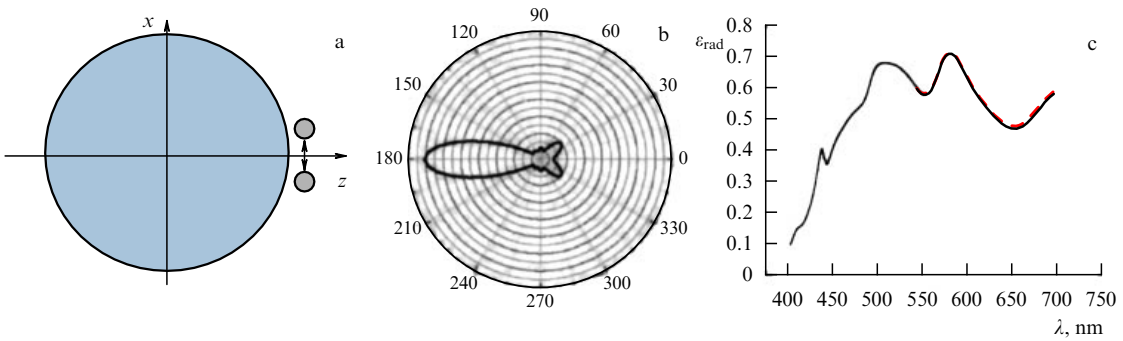

Figure 29. (Color online.) Hybrid metallic–dielectric nanoantenna. (a) Schematic representation. Diameter of dielectric sphere is 500 nm, and material is TiO_2. The system is fed from an emitter (arrow) placed between two silver nanoparticles 60 nm in diameter each; the gap between them measures 8 nm. The entire system is embedded in a matrix having a refraction index of 1.3. (b) Directivity diagram at 525 nm. (c) Radiation efficiency for an ideal emitter and an emitter with substantial internal losses (red dashed and black solid curves, respectively). (Taken from Ref. [158].)

Current investigations of nonlinear optical nanoantennas, including those with adjustable parameters, are categorized into two groups in terms of the mode of achieving nonlinearity. In some of them [69, 123, 185–188], the authors make use of the nonlinear optical response of such metals as silver, gold, and aluminum, i.e., materials from which nanoantennas are made, and the nonlinear dependence of local charge density at the surface of metallic nanoelements on the external optical field strength. In the second group [43, 189–195], the dependence of a conduction current in semiconductors on the strength of the applied electric field is employed.

In Sections 5.1 and 5.2, work on nonlinear and tunable nanoantennas are discussed in greater detail, including studies on optical nonlinearity in nanoantennas themselves. Some publications concerning enhancement of the nonlinear optical response of various materials placed in the strong confinement region of the near field of receiving nanoantennas are considered in Section 6, specially devoted to their practical applications.

5.1 Nonlinear optical response in a metal

Studies on nonlinearity in small (micro- and nanoscale) metallic particles and structures based on them have a rather long history [27, 107, 196–206]. Concrete mechanisms of emerging nonlinearity, discussed in the above publications, are not considered here; instead, we notice that such small metal particles (silver or gold) exhibit an extremely strong linear response. For example, the third-order susceptibility is roughly $\chi^{(3)} \simeq 1$ nm^2 V^{-2}, i.e., much higher than in optical materials showing the highest degree of nonlinearity, such as lithium niobate [27]. Evidently, the use of nonlinear optical response of plasmonic nanoelements extends the potential of photonics in general, and the application of plasmonic nanoantennas in particular.

Control over the dipole moment induced in a plasmonic nanoparticle by varying the external field strength makes it possible to manipulate the directivity diagram of its scattered radiation. This idea was realized in Ref. [69], where the nonlinear response of a hybrid (metallic–dielectric) nanodimer consisting of silver and silicon nanoparticles (Fig. 30a) was employed for switching between the directions of the main lobe of the radiation directivity diagram. The silver nanoparticle is utilized to achieve the nonlinear response, while the silicon nanoparticle breaks the symmetry of the system so that it becomes possible to change the directivity diagram. This line of reasoning is illustrated by Fig. 30b showing radiation scattering diagrams (left and right) in the linear and nonlinear regimes, respectively. The incident radiation wavelength equals 420 nm in both cases. It is indicated in Ref. [69] that the switching effect must be apparent at intensities on the order of 11 MW cm^{-2}, i.e., at quite real and practically attainable values, while the switching time must be 260 fs.

A very interesting paper [185] considers the emergence of the nonlinear optical response in such a seemingly well-known system as a plasmonic nanodimer in a somewhat different manner (Fig. 31). The authors studied the dependence of tunneling current between very close plasmonic nanoparticles on the incident radiation field strength. The dimer is bypassed by the tunneling current that, generally speaking, cannot be neglected when the distance between the charged surfaces of plasmonic nanoparticles is less than 1 nm. This results, in turn, in a decrease in the confined field enhancement factor in the gap of the nanodimer. The

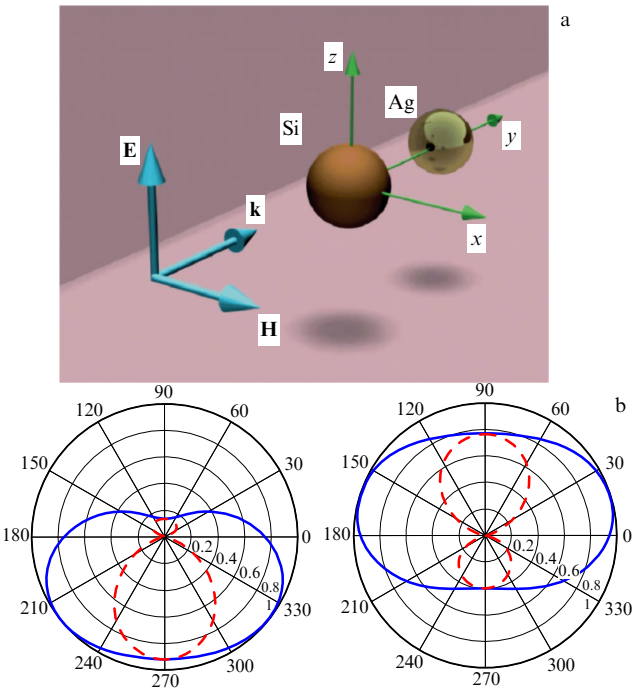

Figure 30. (Color online.) Nonlinear optical metallic–dielectric nanodimer. (a) Problem geometry. The nanodimer is formed from silicon (Si) and silver (Ag) nanoparticles having radii of 30 and 15 nm, respectively. Particle centers are spaced 80 nm apart. Blue arrows indicate the direction of the incident external plane wave and its polarization. (b) Directivity diagrams of scattered radiation at 420 nm in the linear (left) and nonlinear (right) regimes. (Taken from Ref. [69].)

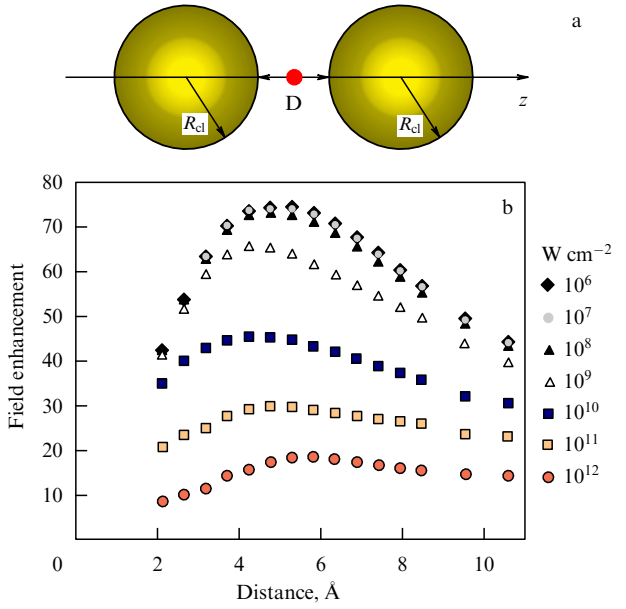

Figure 31. (Color online.) (a) Problem geometry. Symmetric plasmonic nanodimer is considered, and red bold point marks the place for which the confined field enhancement factor is calculated. (b) The set of curves showing the dependence of the confined field enhancement factor on the distance between particle surfaces for different strengths of the external optical field. Confined field strength tends to decrease with increasing external radiation power. Such behavior is related to the effect of bypassing the plasmonic nanodimer by the tunneling current flowing across the nanodimer gap. (Taken from Ref. [185].)

tunneling current essentially depends on the charge density at the particle surface that, in turn, shows dependence on the external optical field strength and the type of the eigenmode excited in the plasmonic nanodimer. This leads to a decrease in the electric field confinement factor in the gap of the nanodimer if the external field strength increases. It is worthy of note, however, that the 'gel' model employed in simulating the behavior of an electron gas in metals from which the dimer is formed cannot be used to elucidate the dependence of the tunneling current on the type of metal — it is universal. Nor does this model allow considering the influence of the intrinsic nonlinearity of the metal (e.g., gold) that prevails over the nonlinearity introduced by tunneling currents at the field strengths employed by the authors.

5.2 Nonlinear optical response in a semiconductor

Semiconductors make up another class of materials utilized to achieve the nonlinear response of nanoantennas [43, 189–195, 207]. The authors of the first publication devoted to this issue [191] proposed using the dependence of the generation of free charge carriers (electrons and holes) in semiconductors on the applied electric field for setting the radiation parameters of nanoantennas. Obviously, the size of semiconductor nanocrystals being extremely small, the field strength must be very high to induce the nonlinear response. These conditions are fulfilled in the gaps of dipole or bowtie nanoantennas. Figure 32 presents the design of such a nonlinear nanoantenna in the form of a dipole with a small semiconducting amorphous silicon nanocrystal inserted in its gap. After such a nonlinear dipole is placed in the external optical field, the semiconducting crystal maintains the passage of current bypassing the dipole. The current value is a function of the field strength in the semiconducting crystal, which, in turn, depends on the type of mode excited in the system. Figure 32a, b shows two states of such a system. Figure 32a corresponds to a dipole eigenmode creating a strong field in the gap. In this case, the high current in the semiconducting crystal runs opposite to the current in the dipole arms. The authors regard this state of the device as closed. Figure 32b illustrates the opposite situation in which the current across the dipole gap is codirectional with the current in the arms. In this case, the condition of half-wave resonance along the entire dipole length is fulfilled, and the system begins to emit (and absorb) radiation more efficiently. The ratio between extinction coefficient maxima corresponding to the open and closed states equals 2.

The above method for the introduction of optical nonlinearity into nanoantennas was extended to plasmonic Yagi–Uda nanoantennas in Ref. [43]. The design is sketched in Fig. 33. Here, the nonlinear nanodipole of the geometry resembling in general that of the dipole described in the preceding paragraph is supplemented with a few more plasmonic nanoelements. The resultant geometry corresponds to the design of a Yagi–Uda nanoantenna with an active vibrator, the gap of which is filled with a semiconducting material, e.g., amorphous silicon. The authors demonstrated the possibility of controling the operational characteristics of such a device by varying external optical field strength.

To sum up, the development of nanoantennas with adjustable working parameters is highly desirable for the reasons described in the introduction to the present section.

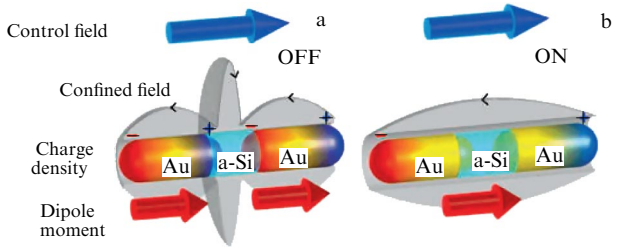

Figure 32. Design of a nonlinear optical dipole. The nanoantenna comprises a dipole with an amorphous silicon nanocrystal inserted in the gap between its arms. The crystal is needed to achieve the nonlinear response of the whole dipole. Figures (a) and (b) show the distributions of charge density and confined field along the length of the dipole in the OFF and ON states, respectively. (Taken from Ref. [191].)

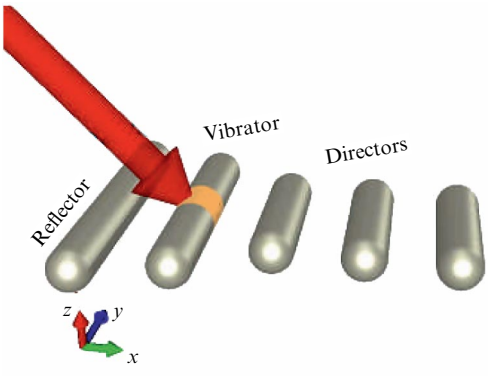

Figure 33. (Color online) Design of a tunable optical Yagi–Uda nanoantenna. Operational regime is adjusted by external radiation (large arrow). (Taken from Ref. [43].)

6. Application of optical nanoantennas

Optical antennas may find application in various spheres of human activity, such as medicine, photovoltaics, spectroscopy, near-field microscopy, and photonics. Some of them already employ optical antennas in actually operating devices (spectroscopy), while others are expected to start using them in the near future (medicine). Another fields (e.g., photovoltaics and photonics) are still experimental test sites with nanoantennas. Applications of optical nanoantennas in medicine for diagnostics and the treatment of malignant tumors are considered in Section 6.1, ways of improving the efficiency of solar cells in Section 6.2, the use of antennas for the enlargement of Raman scattering cross sections in Section 6.3, and their application in the capacity of specialized probes for near-field microscopy in Section 6.4.

6.1 Medicine

Effective therapy for malignant neoplasms is a major unresolved challenge in modern medicine. It may be addressed by utilizing metallic nanoparticles, e.g., metal nanoshells introduced at the affected site to be irradiated with the near-infrared light. Radiation causes heating of nanoparticles [208] which transfer the heat to cancer cells and thereby kill them. This approach began to be developed in the 1990s in studies by N J Halas and co-workers on the optical properties of metal nanoshells [209]. Today, this method is employed in the experimental treatment of malignancies in mice [210]. Strictly speaking, this practice

cannot be regarded as the application of optical antennas, because it is based on the heating of metallic nanoparticles by absorbed light (the parasitic effect in nanoantennas). At the same time, current trends in this research area suggest the employment of complex particles (nanocomplexes), allowing the cancer cells not only to be heated but also to be visualized with the aid of enhanced fluorescence microscopy [210] (see Section 6.4 for details).

6.2 Photovoltaics

The main problem facing modern solar power engineering is the development of thin-film solar cells efficiently converting solar radiation to electric current and significantly reducing the cost of the electric power thus produced, which is presently 2–3 times that of the power generated by other sources [211]. The employment of thin photosensitive films in solar cells may decrease the cost of electric power by an order of magnitude compared with current values due not only to the reduced consumption of refined semiconductors per unit cell area but also to the possibility of fabricating ultrathin (less than 1 μm) semiconducting films on organic and/or polymer substrates by roll-to-roll processing. The price of a solar panel thus obtained per square meter is already competitive on wholesale electricity market; it can be expected to further decrease with increasing power production volume for solar batteries [212].

One of the essential factors hampering further progress in widespread solar power generation is the huge amount of toxic wastes formed in high-purity semiconductor manufacturing processes. A decrease in the thickness of the light-absorbing layer including p–n transition down to 200–300 nm in silicon and GaAs-based cells or even to 100–150 nm in copper-indium-gallium selenide (CIGS) batteries would ensure an environmentally friendly amount of waste, even if solar panels were universally applied [211]. However, absorption of incident light by such thin photosensitive layers can hardly be sufficiently effective. The employment of antireflection coatings to achieve high-efficiency absorption in ordinary solar cells is impracticable in thin-film batteries, because it is necessary not only to compensate for reflection of light but also to prevent its passage through the optically thin photoabsorbing layer. A large part of the solar energy incident on a battery is not simply lost during the passage but is spent on deleterious heating for the photoeffect. Taken together, these factors significantly slow down industrial production of ultrathin film-based solar cells [213].

The application of nanoantennas may significantly promote a solution to this problem. As mentioned above, receiving nanoantennas may confine incident radiation in the subwavelength range. Successful confinement of sunlight is known to prevent both the reflection of incident waves from the battery surface and its passage through the photosensitive layer. These operating conditions are realizable at a few frequencies, so that incident light confinement occurs within essential part of the solar battery working range. Nanoantenna arrays capable of confining incident light inside an optically thin photosensitive layer are called light-trapping nanostructures [173–177, 213, 214]. It is easy to create such arrays, even over a large area on the surface of the light-absorbing layer by deposition methods and nanoimprint lithography [213]. Spinelli et al. [215] overview recent progress in light concentration by trapping nanostructures for thin-film solar cells.

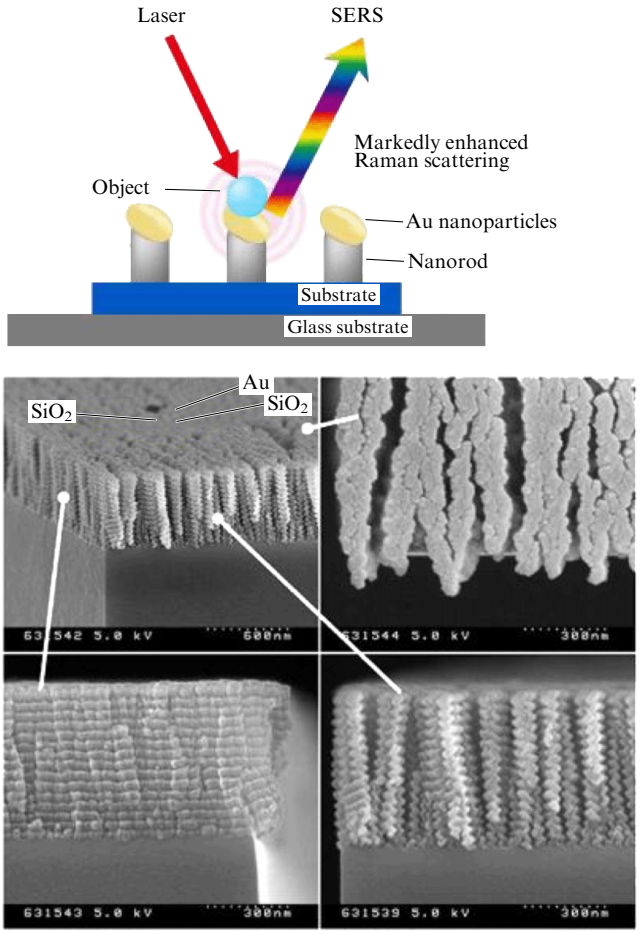

Figure 34. Gold nanoparticles-based SERS substrates manufactured by deposition methods (images taken from Nidek Co. website (http://www.nidek-intl.com). SERS — surface enhanced Raman spectroscopy.

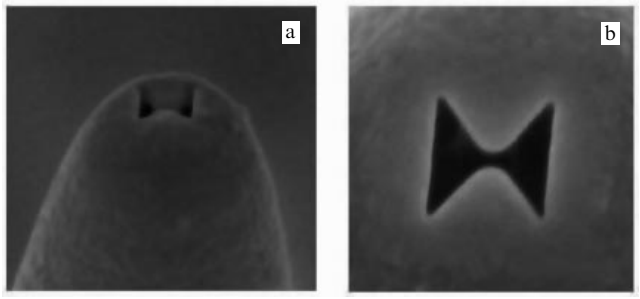

Figure 35. A near-field probe with a bowtie diaphragm has a better signal-to-noise ratio than classical round subwavelength diaphragms. The bowtie diaphragm is shaped by focused ion-beam milling. (Taken from Ref. [224].)

6.3 Spectroscopy

The phenomenon of a giant surface enhanced Raman scattering (SERS) consists in enlargement of the Raman scattering cross section of molecules located near a rough metal surface [23, 216–223]. It was observed for the first time in an experiment as early as the 1970s, and fairly well studied both experimentally and theoretically by the 1980s; several review articles have been published in this time [216, 217]. The practical application of this effect for the creation of substrates to study biological samples required control over rough surfaces with nanoscale accuracy, i.e., the construction of optical antenna arrays. Therefore, the principle objective

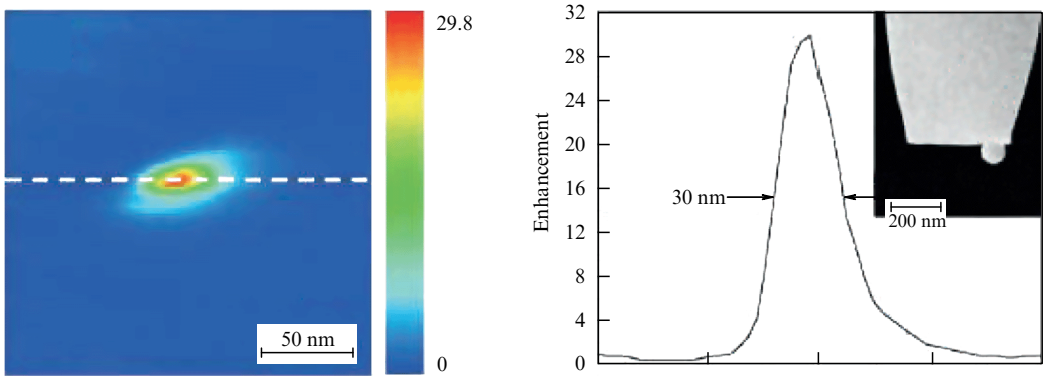

Figure 36. Near-field gold nanosphere-based probe used in experiments on observing enhanced fluorescent scattering by solitary organic molecules. (Taken from Ref. [227].)

of current investigations in this area reduces to searching for the methods of wholesale manufacture of substrates with reproducible properties; they are reviewed in Ref. [222]. Specifically, deposition techniques are applied to commercially produce gold nanoparticle-based SERS substrates (Fig. 34).

6.4 Near-field microscopy

Optical nanoantennas may find application as specialized probes in near-field microscopy and spectroscopy. Classical near-field probes take advantage of light passage through a subwavelength diaphragm (aperture probes) or the effect of electromagnetic field enhancement near the tip of a metal needle (apertureless probes). The design of near-field probes based on optical antennas is extremely complicated; sometimes, it is impossible to distinguish among them on the basis of the presence or absence of an aperture. We shall try to classify probe antennas according to their mode of functioning, viz. giant light transmittance, enhanced fluorescent scattering, giant Raman scattering, and nonlinear optical effects. Optical antennas permit us to dramatically increase the efficiency of light passage through subwavelength diaphragms. Experimentally studied characteristics of bowtie-based probes were reported in Ref. [224] (Fig. 35). It was shown that such probes permit increasing the signal-to-noise ratio by two orders of magnitude over round-aperture probes with the image resolution of $\lambda/20$.

Much work on probe antennas is focused on enhanced fluorescent scattering of solitary molecules or quantum dot emission as the antenna is approached. These effects were observed when using probes based on metallic nanospheres [225–227], nanorods [228], and bowties [116]. For example, paper [227] reports an experimentally found fluorescence enhancement coefficient of 30 and resolution of 20 nm for gold nanosphere-based probes on solitary organic molecules (Fig. 36).

Optical probe antennas are also used in tip-enhanced Raman spectroscopy (TERS) by analogy with a giant SERS near rough metal surfaces. Probe antennas employed in Raman spectroscopy have rather complicated structures, e.g., a combination of a photonic crystal and a plasmonic waveguide [146, 147], co-axial structures [229], and carbon nanotube-based probes [230]. The ability of optical antennas to generate strong confined electromagnetic fields may be exploited to enhance Raman scattering by $10^5 - 10^6$ times and thereby to enable its detection on molecular monolayers [146] (Fig. 37).

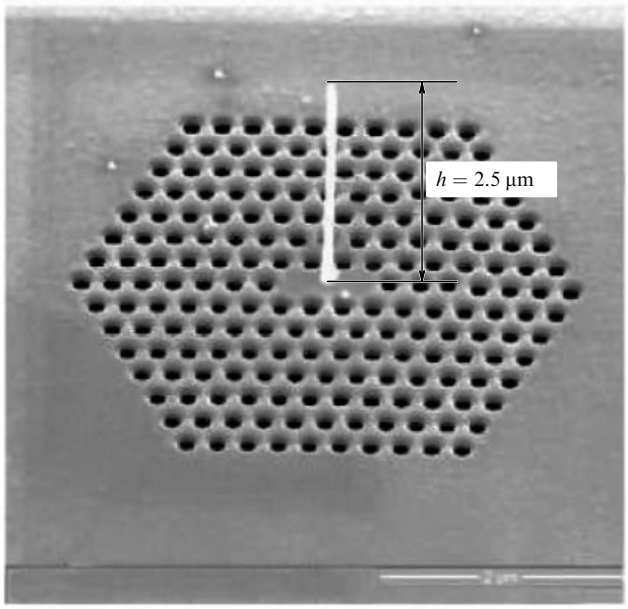

Figure 37. Probe antenna based on the combination of a photon crystal and plasmonic waveguide for conducting giant TERS experiments. The photonic crystal was obtained by focused ion-beam milling, and the plasmonic waveguide by the electron beam-induced gas-phase deposition of metal. (Taken from Ref. [146]).

Optical antennas make it possible to generate a nonlinear optical response [75, 128, 185, 187, 188, 190, 195, 199, 201, 202, 204, 231, 232]. For example, Palomba and Novotny [231] report experimental observation of two-photon luminescence and four-wave mixing in optical nanoantennas formed from pairs of gold spheres 80 nm in diameter (Fig. 38). When such structures serve as near-field probes, four-wave mixing near the junction of nanospheres allows significantly improving the image resolution.

7. Conclusion

The present review undergoes an analysis of the general state of nanoantenna science. Its primary objective is to classify a great variety of nanoantennas into a few types differing in the physical principles behind their functioning. We categorized nanoantennas into two groups, metallic and dielectric, and

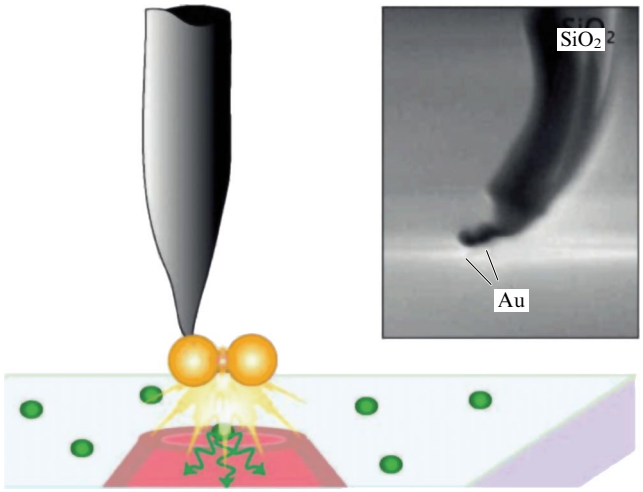

Figure 38. Optical antennas based on gold nanosphere pairs make it possible to observe the nonlinear optical response of the four-wave mixing resulting in field confinement near the junction of nanospheres. (Taken from Ref. [231].)

considered the most typical technical solutions for each group. This is the first attempt at such systematization.

It should be noted to sum up the above discussion that this research area as a part of nano-optics is currently one of the most rapidly developing scientific disciplines. This fact is attributable to the prospects of the great benefits expected from numerous applications of nanoantennas: from biology and medicine, having a need for high-resolution cell microscopy and cancer therapy, to the fabrication of nanophotonic components and devices which, by the most conservative estimate, may improve the performance of modern computing machines by several orders of magnitude. However, the scientific community's interest in optical nanoantennas is not limited to the quest for their fabrication technologies; it also arises from their theoretical and epistemic value. On the one hand, the studies of optical nanoantennas are best suited to reveal the principle of Maxwell equations, implying that technologies commonly used in one area may be transferred after certain modification to another, e.g., from the radio frequency to the visible frequency range. This is the essence of unity between electromagnetism and optics.

On the other hand, nanoantennas constitute devices that cannot be described comprehensively without recourse to quantum mechanics. This is especially true as regards interactions between a quantum emitter and nanoantenna elements, resulting notably in variation of the spontaneous emission rate. This issue has also been reflected in the present review.

Today, it is premature to speak of the widespread intrusion of nanoantennas, but many promising applications are already at the point of being introduced in a clear and practical way, as shown in the review. We hope that its publication will be useful for specialists engaged in studies of optical nanoantennas and interesting for readers unfamiliar with the subject.

Acknowledgments

This work was supported by the Russian Government Program 'The State Support of Research under the Guidance of Leading Scientists at Institutions of Higher Professional Education' (contract No. 11.G34.31.0020 of 28 November 2010) and the governmental Order to Higher Education Institutes (No. 01201259765); it was also supported by the Russian Federation Ministry of Education and Science (agreements No. 11.519.11.2037, No. 14.B37.21.0303, No. 14.132.21.1678), RFBR (grants 13-02-01331A, 13-02-00623A), the Dinastiya Foundation, and the Australian Research Council.

References

1. Silver S *Microwave Antenna*: *Theory and Design* (New York: McGraw-Hill Book Co., 1949)
2. Schelkunoff S A, Friis H T *Antennas*: *Theory and Practice* (New York: Wiley, 1952) [Translated into Russian: *Antenny. Teoriya i Praktika* (Moscow: Sov. Radio, 1955)]
3. Aizenberg G Z *Antenny Ul'trakorotkikh Voln* (Ultrashort Wave Antennas) (Moscow: Svyaz'izdat, 1957)
4. Nadenenko S I *Antenny* (Antennas) (Moscow: Svyaz'izdat, 1959)
5. Markov G T, Sazonov D M *Antenny* (Antennas) (Moscow: Energiya, 1975)
6. Balanis C A *Antenna Theory*: *Analysis and Design* (New York: Harper & Row, 1982)
7. Ulaby F T, Moore R K, Fung A K *Microwave Remote Sensing*: *Active and Passive* Vol. 1 *Microwave Remote Sensing, Fundamentals and Radiometry* (Reading, Mass.: Addison-Wesley Publ. Co., 1981)
8. Ulaby F T, Moore R K, Fung A K *Microwave Remote Sensing*: *Active and Passive* Vol. 2 *Radar Remote Sensing and Surface Scattering and Emission Theory* (Reading, Mass.: Addison-Wesley Publ. Co., 1982)
9. Ulaby F T, Moore R K, Fung A K *Microwave Remote Sensing*: *Active and Passive* Vol. 3 *From Theory to Applications* (Reading, Mass.: Addison-Wesley Publ. Co., 1986)
10. Bond E J et al. *IEEE Trans. Antennas Propag.* **51** 1690 (2003)
11. Maier S A, Atwater H A *J. Appl. Phys.* **98** 011101 (2005)
12. Ozbay E *Science* **311** 189 (2006)
13. Zia R et al. *Mater. Today* **9** (7–8) 20 (2006)
14. van Hulst N F *Nature* **448** 141 (2007)
15. Akimov A V et al. *Nature* **450** 402 (2007)
16. Klimov V V *Phys. Usp.* **51** 839 (2008) [*Usp. Fiz. Nauk* **178** 875 (2008)]
17. Stewart M E et al. *Chem. Rev.* **108** 494 (2008)
18. Klimov V *Nanoplasmonics* (Singapore: Pan Stanford Publ., 2011) [Translated from Russian: *Nanoplazmonika* (Moscow: Fizmatlit, 2010)]
19. MacDonald K F, Zheludev N I *Laser Photon. Rev.* **4** 562 (2010)
20. Stockman M I *Opt. Express* **19** 22029 (2011)
21. Benson O *Nature* **480** 193 (2011)
22. Maier S A *Plasmonics*: *Fundamentals and Applications* (New York: Springer, 2007)
23. Kneipp K, Moskovits M, Kneipp H (Eds) *Surface-Enhanced Raman Scattering*: *Physics and Applications* (Berlin: Springer, 2006)
24. Novotny L, Hecht B *Principles of Nano-Optics* (Cambridge: Cambridge Univ. Press, 2006)
25. Alù A, Engheta N *Nature Photon.* **2** 307 (2008)
26. Novotny L *Nature* **455** 887 (2008)
27. Bharadwaj P, Deutsch B, Novotny L *Adv. Opt. Photon.* **1** 438 (2009)
28. Novotny L, van Hulst N *Nature Photon.* **5** 83 (2011)
29. Curto A G et al. *Science* **329** 930 (2010)
30. Dregely D et al. *Nature Commun.* **2** 267 (2011)
31. Cao L et al. *Nano Lett.* **10** 439 (2010)
32. Cao L et al. *Nano Lett.* **10** 1229 (2010)
33. Lerosey G *Nature Photon.* **4** 267 (2010)
34. Krasnok A E et al. *JETP Lett.* **94** 593 (2011) [*Pis'ma Zh. Eksp. Teor. Fiz.* **94** 635 (2011)]
35. Dorfmüller J et al. *Nano Lett.* **11** 2819 (2011)
36. Shegai T et al. *Nature Commun.* **2** 481 (2011)
37. Giannini V et al. *Chem. Rev.* **111** 3888 (2011)
38. Maksymov I S, Miroshnichenko A E *Opt. Express* **19** 5888 (2011)
39. Maksymov I S, Davoyan A R, Kivshar Yu S *Appl. Phys. Lett.* **99** 083304 (2011)
40. de la Chapelle M L, Pucci A (Eds) *Nanoantenna*: *Plasmon-Enhanced Spectroscopies for Biotechnological Applications* (Singapore: Pan Stanford Publ., 2012)

41. Biagioni P, Huang J-S, Hecht B *Rep. Prog. Phys.* **75** 024402 (2012)
42. Filonov D S et al. *Appl. Phys. Lett.* **100** 201113 (2012)
43. Maksymov I S, Miroshnichenko A E, Kivshar Yu S *Opt. Express* **20** 8929 (2012)
44. Olmon R L, Raschke M B *Nanotechnology* **23** 444001 (2012)
45. DasGupta D et al. *Appl. Phys. Lett.* **95** 233701 (2009)
46. Kim K et al. *J. Controlled Release* **146** 219 (2010)
47. Chanda N et al. *Nanomed. Nanotechnol. Biol. Med.* **6** 201 (2010)
48. Cai W et al. *Nanotechnol. Sci. Appl.* **1** 17 (2008)
49. Rai M, Duran N (Eds) *Metal Nanoparticles in Microbiology* (Berlin: Springer-Verlag, 2011)
50. Huang X, Neretina S, El-Sayed M A *Adv. Mater.* **21** 4880 (2009)
51. Chan W S W (Ed.) *Bio-Applications of Nanoparticles* (New York: Springer Science + Business Media, 2007)
52. Hanafi N *Int. J. Res. Biol. Sci.* **2** 6 (2012)
53. Cho Y W et al. *Biomaterials* **28** 1236 (2007)
54. Cho Y W et al. *Macromol. Res.* **16** 15 (2008)
55. Liang M et al. *Bioconjugate Chem.* **21** 1385 (2010)
56. Klimov V V *JETP Lett.* **78** 471 (2003) [*Pis'ma Zh. Eksp. Teor. Fiz.* **78** 943 (2003)]
57. Guzatov D V, Klimov V V *Quantum Electron.* **35** 891 (2005) [*Kvantovaya Elektron.* **35** 891 (2005)]
58. Denisyuk A I *J. Opt. Technol.* **77** 527 (2010) [*Opt. Zh.* **77** (9) 3 (2010)]
59. Slyusar D, Slyusar V *Elektron. Nauka Tekhnol. Bizness* (6) 74 (2011)
60. Baryshev A V, Eremin Yu A *Komp'yut. Opt.* **35** 311 (2011)
61. Slyusar V *Elektron. Nauka Tekhnol. Bizness* (2) 58 (2009)
62. Lagarkov A N et al. *Phys. Usp.* **52** 959 (2009) [*Usp. Fiz. Nauk* **179** 1018 (2009)]
63. Shalin A S, Sukhov S V *Quantum Electron.* **42** 355 (2012) [*Kvantovaya Elektron.* **42** 355 (2012)]
64. Zabkov I V et al. *Quantum Electron.* **41** 742 (2011) [*Kvantovaya Elektron.* **41** 742 (2011)]
65. Klimov V V, Guzatov D V *Phys. Usp.* **55** 1054 (2012) [*Usp. Fiz. Nauk* **182** 1130 (2012)]
66. Klimov V V, Ducloy M *Phys. Rev. A* **69** 013812 (2004)
67. Guzatov D V, Klimov V V *Phys. Rev. A* **75** 052901 (2007)
68. Klimov V V, Guzatov D V *Phys. Rev. B* **75** 024303 (2007)
69. Noskov R E, Krasnok A E, Kivshar Yu S *New J. Phys.* **14** 093005 (2012)
70. Krasnok A E et al. *Opt. Express* **20** 20599 (2012)
71. Vladimirova Yu V et al. *Phys. Rev. A* **85** 053408 (2012)
72. Guzatov D V, Klimov V V *New J. Phys.* **13** 053034 (2011)
73. Klimov V V, Guzatov D V *Appl. Phys. A* **89** 305 (2007)
74. Krasnok A E et al. *AIP Conf. Proc.* **1475** 22 (2012)
75. Lapshina N, Noskov R, Kivshar Yu *Opt. Lett.* **37** 3921 (2012)
76. Kuznetsov A I et al. *Sci. Rep.* **2** 492 (2012)
77. Miroshnichenko A E et al. *Phys. Status Solidi RRL* **5** 347 (2011)
78. Maksymov I S, Miroshnichenko A E, Kivshar Yu S *Phys. Rev. A* **86** 011801(R) (2012)
79. Wessel J *J. Opt. Soc. Am. B* **2** 1538 (1985)
80. Novotny L *Phys. Today* **64** (7) 47 (2011)
81. Vinogradov A P et al. *Phys. Usp.* **55** 1046 (2012) [*Usp. Fiz. Nauk* **182** 1122 (2012)]
82. Maier S A et al. *Nature Mater.* **2** 229 (2003)
83. Pile D F P et al. *Appl. Phys. Lett.* **87** 261114 (2005)
84. Liu L, Han Z, He S *Opt. Express* **13** 6645 (2005)
85. Matsuzaki Y et al. *Opt. Express* **16** 16314 (2008)
86. Oulton R F et al. *Nature Photon.* **2** 496 (2008)
87. Novotny L, Bian R X, Xie X S *Phys. Rev. Lett.* **79** 645 (1997)
88. Xu H et al. *Phys. Rev. Lett.* **83** 4357 (1999)
89. Li K, Stockman M I, Bergman D J *Phys. Rev. Lett.* **91** 227402 (2003)
90. Ahmadi A, Mosallaei H *Opt. Lett.* **35** 3706 (2010)
91. Grosjean T et al. *Nano Lett.* **11** 1009 (2011)
92. Landau L D, Lifshitz E M *Quantum Mechanics: Non-Relativistic Theory* (Oxford: Pergamon Press, 1977) [Translated from Russian: *Kvantovaya Mekhanika: Nerelyativistskaya Teoriya* (Moscow: Nauka, 1974)]
93. Purcell E M *Phys. Rev.* **69** 681 (1946)
94. Noda S, Fujita M, Asano T *Nature Photon.* **1** 449 (2007)
95. Khitrova G et al. *Nature Phys.* **2** 81 (2006)
96. Saunders W A et al. *J. Appl. Phys.* **72** 806 (1992)
97. Barthes J et al. *Phys. Rev. B* **84** 073403 (2011)
98. Hamam R E et al. *Opt. Express* **16** 12523 (2008)
99. Iorsh I et al. *Phys. Lett. A* **376** 185 (2012)
100. Kidwai O, Zhukovsky S V, Sipe J E *Opt. Lett.* **36** 2530 (2011)
101. del Valle E et al. *New J. Phys.* **13** 113014 (2011)
102. Yablonovitch E, Gmitter T J, Bhat R *Phys. Rev. Lett.* **61** 2546 (1988)
103. Glazov M M et al. *Phys. Solid State* **53** 1753 (2011) [*Fiz. Tverd. Tela* **53** 1665 (2011)]
104. Acuna G P et al. *Science* **338** 506 (2012)
105. Jakubczyk T et al. *Appl. Phys. Lett.* **101** 132105 (2012)
106. Acar H et al. *ACS Nano* **6** 8226 (2012)
107. Ghenuche P et al. *Phys. Rev. Lett.* **101** 116805 (2008)
108. Huang J-S et al. *Nano Lett.* **9** 1897 (2009)
109. Andryieuski A et al. *Opt. Lett.* **37** 1124 (2012)
110. Fang Z et al. *Nano Lett.* **11** 1676 (2011)
111. Alù A, Engheta N *Phys. Rev. B* **78** 195111 (2008)
112. Alù A, Engheta N *Phys. Rev. Lett.* **101** 043901 (2008)
113. Fromm D P et al. *Nano Lett.* **4** 957 (2004)
114. González F J, Boreman G D *Infrared Phys. Technol.* **46** 418 (2005)
115. Schuck P J et al. *Phys. Rev. Lett.* **94** 017402 (2005)
116. Farahani J N et al. *Nanotechnology* **18** 125506 (2007)
117. Yu N et al. *Opt. Express* **15** 13272 (2007)
118. Guo H et al. *Opt. Express* **16** 7756 (2008)
119. Kinkhabwala A et al. *Nature Photon.* **3** 654 (2009)
120. Zhang Z et al. *Nano Lett.* **9** 4505 (2009)
121. Berrier A et al. *Opt. Express* **18** 23226 (2010)
122. Hatab N A et al. *Nano Lett.* **10** 4952 (2010)
123. Ko K D et al. *Nano Lett.* **11** 61 (2011)
124. Rosa L, Sun K, Juodkazis S *Phys. Status Solidi RRL* **5** 175 (2011)
125. Sederberg S, Elezzabi A Y *Opt. Express* **19** 15532 (2011)
126. Kang T et al. *Nano Lett.* **12** 2331 (2012)
127. Roxworthy B J et al. *Nano Lett.* **12** 796 (2012)
128. Suh J Y et al. *Nano Lett.* **12** 269 (2012)
129. Volpe G, Volpe G, Quidant R *Opt. Express* **19** 3612 (2011)
130. Li J, Salandrino A, Engheta N *Phys. Rev. B* **76** 245403 (2007)
131. Pakizeh T, Kall M *Nano Lett.* **9** 2343 (2009)
132. Taminiau T H, Stefani F D, van Hulst N F *Opt. Express* **16** 10858 (2008)
133. Li J, Salandrino A, Engheta N *Phys. Rev. B* **79** 195104 (2009)
134. Stout B et al. *J. Opt. Soc. Am. B* **28** 1213 (2011)
135. Coenen T et al. *Nano Lett.* **11** 3779 (2011)
136. Bonod N et al. *Phys. Rev. B* **82** 115429 (2010)
137. Kosako T, Kadoya Y, Hofmann H F *Nature Photon.* **4** 312 (2010)
138. Hofmann H F, Kosako T, Kadoya Y *New J. Phys.* **9** 217 (2007)
139. Lobanov S V et al. *Phys. Rev. B* **85** 155137 (2012)
140. Sengupta D L *IRE Trans. Antennas Propagat.* **8** 11 (1960)
141. Simovski C, Luukkonen O *Opt. Commun.* **285** 3397 (2012)
142. Boriskina S V, Dal Negro L *Opt. Lett.* **35** 538 (2010)
143. Staude I et al. *Phys. Status Solidi RRL* **6** 466 (2012)
144. Ramaccia D et al. *Opt. Lett.* **36** 1743 (2011)
145. Iluz Z, Boag A *Opt. Lett.* **36** 2773 (2011)
146. De Angelis F et al. *Nano Lett.* **8** 2321 (2008)
147. De Angelis F et al. *Nature Nanotechnol.* **5** 67 (2010)
148. Maksymov I S et al. *Opt. Commun.* **285** 821 (2012)
149. Mironov V L *Osnovy Skaniruyushchei Zondovoi Mikroskopii* (Fundamentals of Scanning Probe Microscopy) (Nizhny Novgorod: Inst. Fiziki Mikrostruktur RAN, 2004)
150. Pavlov R S, Curto A G, van Hulst N F *Opt. Commun.* **285** 3334 (2012)
151. Navarro-Cia M, Maier S A *ACS Nano* **6** 3537 (2012)
152. Giannini V, Sánchez-Gil J A *Opt. Lett.* **33** 899 (2008)
153. Lee H et al. *Nano Lett.* **11** 119 (2011)
154. Shegai T et al. *Nano Lett.* **12** 2464 (2012)
155. Klemm M *Int. J. Opt.* **2012** 348306 (2012)
156. Boriskina S V, Reinhard B M *Proc. Natl. Acad. Sci. USA* **108** 3147 (2011)
157. Boriskina S V, Reinhard B M *Opt. Express* **19** 22305 (2011)
158. Devilez A, Stout B, Bonod N *ACS Nano* **4** 3390 (2010)
159. Devilez A et al. *Opt. Express* **17** 2089 (2009)
160. Pellegrini G, Mattei G, Mazzoldi P *ACS Nano* **3** 2715 (2009)
161. Gérard D et al. *J. Opt. Soc. Am. B* **26** 1473 (2009)
162. Walker B N et al. *J. Phys. Chem. C* **114** 4835 (2010)
163. Mendes M J et al. *Opt. Express* **19** 16207 (2011)
164. Yang S, Taflove A, Backman V *Opt. Express* **19** 7084 (2011)
165. Cao L, Fan P, Brongersma M L *Nano Lett.* **11** 1463 (2011)

166. Lee K G et al. *Nature Photon.* **5** 166 (2011)
167. Wu J et al. *Phys. Rev. B* **81** 165415 (2010)
168. Zhuo R F et al. *J. Appl. Phys.* **104** 094101 (2008)
169. Rolly B, Stout B, Bonod N *Opt. Express* **20** 20376 (2012)
170. Liu Y G et al. *Opt. Lett.* **37** 2112 (2012)
171. Liu W et al. *ACS Nano* **6** 5489 (2012)
172. Evlyukhin A B et al. *Phys. Rev. B* **82** 045404 (2010)
173. Fahim N F et al. *Opt. Express* **20** A694 (2012)
174. Trompoukis C et al. *Appl. Phys. Lett.* **101** 103901 (2012)
175. Yu Y et al. *Nano Lett.* **12** 3674 (2012)
176. Mavrokefalos A et al. *Nano Lett.* **12** 2792 (2012)
177. Jeong S et al. *Nano Lett.* **12** 2971 (2012)
178. Boriskina S V, Reinhard B M *Nanoscale* **4** 76 (2012)
179. Merchiers O et al. *Phys. Rev. A* **76** 043834 (2007)
180. Ginn J C et al. *Phys. Rev. Lett.* **108** 097402 (2012)
181. Wang J et al. *J. Appl. Phys.* **111** 044903 (2012)
182. Němec H et al. *Appl. Phys. Lett.* **100** 061117 (2012)
183. Stratton J A *Electromagnetic Theory* (New York: McGraw-Hill, 1941)
184. Palik E D (Ed.) *Handbook of Optical Constants of Solids* (New York: Academic Press, 1985)
185. Marinica D C et al. *Nano Lett.* **12** 1333 (2012)
186. Abb M et al. *Nano Lett.* **11** 2457 (2011)
187. Castro-Lopez M et al. *Nano Lett.* **11** 4674 (2011)
188. Schumacher T et al. *Nature Commun.* **2** 333 (2011)
189. Chen P-Y, Alù A *Phys. Rev. B* **82** 235405 (2010)
190. Harutyunyan H et al. *Phys. Rev. Lett.* **108** 217403 (2012)
191. Large N et al. *Nano Lett.* **10** 1741 (2010)
192. Palpant B, in *Non-linear Optical Properties of Matter*: *From Molecules to Condensed Phases* (Eds M G Papadopoulos, A J Sadlej, J Leszczynski) (Dordrecht: Springer, 2006)
193. Lippitz M, van Dijk M A, Orrit M *Nano Lett.* **5** 799 (2005)
194. Danckwerts M, Novotny L *Phys. Rev. Lett.* **98** 026104 (2007)
195. Zhou F et al. *Opt. Express* **18** 13337 (2010)
196. Hache F et al. *Appl. Phys. A* **47** 347 (1988)
197. Rautian S G *JETP* **85** 451 (1997) [*Zh. Eksp. Teor. Fiz.* **112** 836 (1997)]
198. Drachev V P et al. *Nano Lett.* **4** 1535 (2004)
199. Zharov A A, Noskov R E, Tsarev M V *J. Appl. Phys.* **106** 073104 (2009)
200. Noskov R E, Zharov A A, Tsarev M V *Phys. Rev. B* **82** 073404 (2010)
201. Palomba S, Danckwerts M, Novotny L *J. Opt. A* **11** 114030 (2009)
202. Ren M et al. *Nature Commun.* **3** 833 (2012)
203. Bautista G et al. *Nano Lett.* **12** 3207 (2012)
204. Hache F, Ricard D, Girard C *Phys. Rev. B* **38** 7990 (1988)
205. Hache F, Ricard D *J. Phys. Condens. Matter* **1** 8035 (1989)
206. Deal Fatti N D et al. *Chem. Phys.* **251** 215 (2000)
207. Chen P-Y, Alù A *Nano Lett.* **11** 5514 (2011)
208. Tribelsky M I et al. *Phys. Rev. X* **1** 021024 (2011)
209. Averitt R D, Sarkar D, Halas N J *Phys. Rev. Lett.* **78** 4217 (1997)
210. Bardhan R et al. *Acc. Chem. Res.* **44** 936 (2011)
211. Martí A, Luque A *Next Generation Photovoltaics*: *High Efficiency Through Full Spectrum Utilization* (Bristol: Institute of Physics, 2004)
212. "Ultra-low-cost solar electricity cells", http://cache.rmartinr.com/NanosolarCellWhitePaper.pdf (Nanosolar, Inc., White Paper, September 2, 2009)
213. Atwater H A, Polman A *Nature Mater.* **9** 205 (2010)
214. Deceglie M G et al. *Nano Lett.* **12** 2894 (2012)
215. Spinelli P et al. *J. Opt.* **14** 024002 (2012)
216. Moskovits M *Rev. Mod. Phys.* **57** 783 (1985)
217. Emel'yanov V I, Koroteev N I *Sov. Phys. Usp.* **24** 864 (1981) [*Usp. Fiz. Nauk* **135** 345 (1981)]
218. Brolo A G et al. *Nano Lett.* **4** 2015 (2004)
219. Baumberg J J et al. *Nano Lett.* **5** 2262 (2005)
220. Li J F et al. *Nature* **464** 392 (2010)
221. Steuwe C et al. *Nano Lett.* **11** 5339 (2011)
222. Fan M, Andrade G F S, Brolo A G *Analyt. Chim. Acta.* **693** 7 (2011)
223. Li H et al. *J. Phys. Chem. C* **116** 23608 (2012)
224. Vo T-P et al. *Opt. Express* **20** 4124 (2012)
225. Anger P, Bharadwaj P, Novotny L *Phys. Rev. Lett.* **96** 113002 (2006)
226. Höppener C, Novotny L *Nanotechnology* **19** 384012 (2008)
227. Eghlidi H et al. *Nano Lett.* **9** 4007 (2009)
228. Taminiau T H et al. *Nature Photon.* **2** 234 (2008)
229. Weber-Bargioni A et al. *Nano Lett.* **11** 1201 (2011)
230. Kolerov A N *Tech. Phys. Lett.* **37** 259 (2011) [*Pis'ma Zh. Tekh. Fiz.* **37** (6) 33 (2011)]
231. Palomba S, Novotny L *Nano Lett.* **9** 3801 (2009)
232. Abb M et al. *ACS Nano* **6** 6462 (2012)